Review

pubs.acs.org/Biomac

3D Printing Polymers with Supramolecular Functionality for Biological Applications

Allison M. Pekkanen,[†,‡] Ryan J. Mondschein,[‡,∥] Christopher B. Williams,[‡,§] and Timothy E. Long*[,‡,∥]

[†]School of Biomedical Engineering and Sciences, Virginia Tech, Blacksburg, Virginia 24061, United States
[‡]Macromolecules Innovation Institute (MII), Virginia Tech, Blacksburg, Virginia 24061, United States
[§]Department of Mechanical Engineering, Virginia Tech, Blacksburg, Virginia 24061, United States
[∥]Department of Chemistry, Virginia Tech, Blacksburg, Virginia 24061, United States

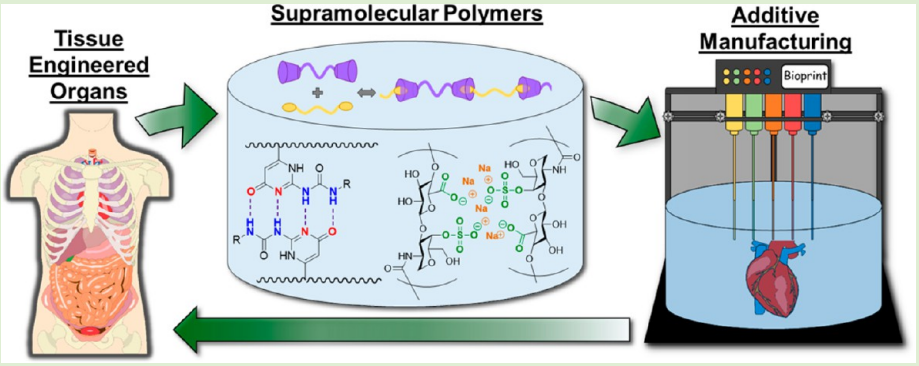

ABSTRACT: Supramolecular chemistry continues to experience widespread growth, as fine-tuned chemical structures lead to well-defined bulk materials. Previous literature described the roles of hydrogen bonding, ionic aggregation, guest/host interactions, and $\pi-\pi$ stacking to tune mechanical, viscoelastic, and processing performance. The versatility of reversible interactions enables the more facile manufacturing of molded parts with tailored hierarchical structures such as tissue engineered scaffolds for biological applications. Recently, supramolecular polymers and additive manufacturing processes merged to provide parts with control of the molecular, macromolecular, and feature length scales. Additive manufacturing, or 3D printing, generates customizable constructs desirable for many applications, and the introduction of supramolecular interactions will potentially increase production speed, offer a tunable surface structure for controlling cell/scaffold interactions, and impart desired mechanical properties through reinforcing interlayer adhesion and introducing gradients or self-assembled structures. This review details the synthesis and characterization of supramolecular polymers suitable for additive manufacture and biomedical applications as well as the use of supramolecular polymers in additive manufacturing for drug delivery and complex tissue scaffold formation. The effect of supramolecular assembly and its dynamic behavior offers potential for controlling the anisotropy of the printed objects with exquisite geometrical control. The potential for supramolecular polymers to generate well-defined parts, hierarchical structures, and scaffolds with gradient properties/tuned surfaces provides an avenue for developing next-generation biomedical devices and tissue scaffolds.

1. INTRODUCTION

The field of polymers who structure and function depends on supramolecular interactions describes an emerging field of polymer chemistry that precisely controls both chemical structure and noncovalent interactions between polymer chains.[1,2] Supramolecular chemistry employs relatively weak interactions between small molecules or polymers to provide a well-defined 2D or 3D structure.[1,3] Supramolecular interactions between polymer chains include ionic interactions, hydrogen bonding, guest/host interactions, and $\pi-\pi$ stacking, each with varying degrees of strength.[2−5] Most supramolecular interactions are relatively weaker than covalent bonds, offering opportunities for a dynamic structure and tunable viscoelastic behavior.[6] Importantly, the reversibility of supramolecular interactions facilitates the manufacturing of an array of objects due to advantageous rheological performance. The ability to disrupt supramolecular bonds during processing affords improved flow properties relative to high molecular weight polymers of similar composition. Reforming interactions postprocessing in the final structure assures the final constructs or parts maintain desired thermomechanical properties. The enhanced processing behavior of supramolecular polymers makes them ideal candidates for additive manufacturing (AM).

AM, also known as 3D printing or rapid prototyping, emerged to generate previously unattainable geometric structures and functions from well-characterized materials

Received: May 11, 2017
Revised: July 27, 2017
Published: August 1, 2017

DOI: 10.1021/acs.biomac.7b00671
Biomacromolecules 2017, 18, 2669−2687

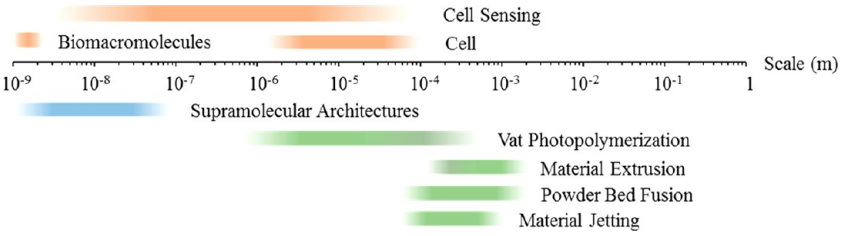

Figure 1. Resolution of common AM techniques fails to reach the breadth of cellular sensing capabilities, necessitating the use of both additive manufacturing and supramolecular interactions to reach control of fine features.[27,35]

developed for traditional processing techniques such as injection/blow molding and extrusion. A large concern with AM arises from slower processing times relative to conventional processing techniques. Certain AM processes also compromise mechanical properties of final parts due to weak interlayer adhesion. Supramolecular polymers offer the ability to overcome both challenges, as the improved processing behavior, as previously mentioned, increases print speeds without jeopardizing final construct properties, and supramolecular interactions also potentially afford improved interlayer adhesion between "weld lines" in constructs.[7,8]

While AM generated new structural geometries composed of existing materials, biology also benefited from the creation of processing techniques that potentially replicates nano-/microscale geometries with high fidelity and precision. This led to the development of novel drug delivery devices and tissue scaffolds.[9] The ability to easily replicate different organs or biological tissue is crucial to develop next-generation medical devices and tissue scaffolds, since no two organs are the same size or shape. Material extrusion AM, vat photopolymerization, and inkjet printing commonly generated novel structures suitable for incorporation into the human body.[10,11] Specifically, the control of not only geometry but also porosity aided in formulation of complex biological structures capable of sustaining cellular viability and proliferation.[12] Furthermore, recent advances in bioprinting allow for cell encapsulation into polymers for simultaneous deposition into complex tissue scaffolds.[13] The combination of supramolecular polymers with biologically relevant hydrogels reveals a promising approach to complex tissue engineering, combining reversible, supramolecular bonds and water to lower the glass transition temperature (T_g) and lend chain mobility.[14,15]

While advances in additive manufacturing open opportunities for new tissue scaffolds, the breadth of cell sensing requires the incorporation of supramolecular functionality to create distinct structures on various length scales (Figure 1). Resolution of common AM techniques, while improving rapidly, remains limited in scope compared to cell sensing capabilities. Tissue engineering involves the replication of native biological tissues *in vitro* for a variety of applications such as drug discovery, disease characterization, and organ replacement.[16] Tissue scaffolds generated from nonspecific molding or precisely tuned 3D structure closely mimic a cell or organ type of choice.[12,17−19] The field of tissue engineering includes both synthetic and natural polymers, lending great diversity to the field.[20−22] Specifically, common tissue engineering constructs closely mimic native cartilage, which is generated from chondrocytes.[23−25] Stem cells, which differentiate into specific tissue types, tune differentiation based on the modulus and chemical environment of the resulting scaffold.[26,27] Recent advances for *in vitro* 3D cell culture include complex tissues such as skin (keratinocytes, fibroblasts),[28] liver (hepatocytes),[29] brain and spinal cord (neurons),[30] blood vessels (endothelial),[31] and heart (aortic valve, smooth muscle),[32] which forge the way for future tissue engineered scaffolds capable of mimicking complete organs.[33,34]

The goal of tissue engineering, i.e. to replicate natural tissue, relies on creating biologically active and hierarchical/gradient structures with well-defined features and surfaces.[36] The control of scale, features, and properties makes AM a perfect processing technique to develop complex tissue scaffolds with the prerequisite parameters. Recently, printing techniques with controlled intensity of light during printing resulted in parts with varying moduli across the final construct.[37] This anisotropic behavior closely mimics the gradients observed in biological tissue. Combining supramolecular polymers with AM expands the current state of tissue engineering scaffold fabrication to better control size, scale, features, modulus, and surfaces compared to traditional processing techniques. Thus, this review describes the use of polymers imbibed with supramolecular functionality, both natural and synthetic, for AM designed for biological applications, both with and without encapsulated cells.

2. SYNTHESIS AND CHARACTERIZATION OF 3D-PRINTABLE SUPRAMOLECULAR POLYMERS

Utilizing both synthetic methods and modifications of naturally occurring biopolymers enabled supramolecular polymers appropriate for AM. The modulus, viscosity, and functionality of supramolecular polymers enables their use in AM.[38] Commonly, naturally occurring polymers possess a high molecular weight, which translates to an inherently viscous polymer solution suitable for material extrusion AM.[39] Interestingly, most modified biopolymers combine with a photocurable group or synthetic copolymer to enhance mechanical integrity upon printing. Alternatively, synthetic polymers offer tunable viscosities and functionality through controlling architecture and monomer selection, expanding the potential printing techniques suitable for tissue scaffolds or drug delivery and eliminating manufacturing limitations. The resulting modulus and physical characteristics of the printed polymers also drive their application, with high modulus materials best for applications such as bone tissue engineering and low modulus materials fit for soft tissue applications.[40,41] Supramolecular functionality, modulus, and viscosity dictate both the AM technique used and resulting biological applications.[42]

Difficulty arises in the characterization of supramolecular polymers due to the dynamic nature of the bonds. Common analytical techniques including nuclear magnetic resonance spectroscopy (NMR)[43,44] and Fourier transform infrared spectroscopy (FTIR)[45] offer insight into bond strength as well as the dynamic behavior. Variable temperature FTIR is commonly used to determine association/disassociation temperatures of hydrogen bonding polymers, such as nucleobase-containing acrylates.[46] Tensile properties afford Young's modulus analysis as well as tensile strength and elongation to break. Typically, polymers with supramolecular

DOI: 10.1021/acs.biomac.7b00671
Biomacromolecules 2017, 18, 2669−2687

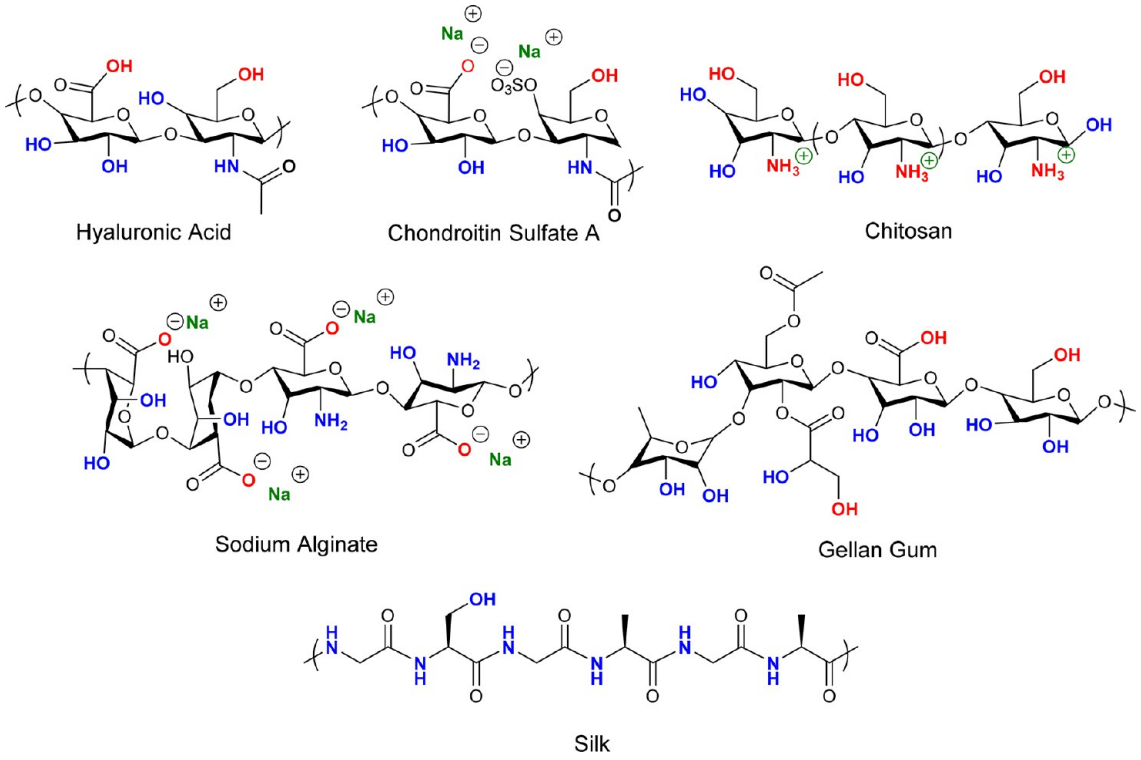

Figure 2. Structures of commonly used natural polymers for AM, including polysaccharides and polypeptides. These biopolymers have been chemically modified (sites marked in red) as well as utilized for their supramolecular behavior either from hydrogen bonding (blue) or ionic (green) interactions.

interactions exhibit enhanced mechanical properties due to the presence of physical cross-links compared to nonassociating analogs.[47] Using interacting end-groups has increased low molecular weight polymer properties to compete with the same composition of high molecular weight for thermoplastic polyesters such as poly(butylene terephthalate)[48] and poly(ethylene glycol) (PEG).[49] Melt or solution rheological analysis also provides insight into polymer chain dynamics and viscoelastic behavior. Frequency or temperature sweeps identify the mechanisms for supramolecular interactions as they restrict or enhance characteristic polymer chain relaxation behavior[7,50,51] as well as supramolecular bond association/disassociation temperatures.[48] Other less common techniques to characterize the influence of supramolecular interactions on polymer properties include X-ray scattering, light scattering, microscopy, and thermal analysis.

2.1. Modifications of Natural Polymers. Naturally occurring polymers or biopolymers offer supramolecular functionality, which while often weaker than synthetic polymers, occurs naturally within the materials.[52] These polymers, however, often necessitate modifications to achieve tailored geometry while printing, such as the inclusion of a photocurable group for direct modification of the biopolymer.[53] Tuning properties of natural polymers remains challenging. These polymers typically exhibit a high amount of orthogonal functionality (H-bonding and ionic interactions), making solubility a concern for chemical modifications or certain printing techniques. Unlike synthetic polymers, difficulty arises in tuning polymer structure and properties through polymerization, as synthesizing natural polymers with common synthetic methods is challenging. Thus, modifying existing natural polymers offers the easiest and most common route to achieve desired properties. Despite the access of many synthetic methods, polymer modification reactions often suffer from limited solubility and viscosity as well as the removal of undesirable side products and less than quantitative yields.

The polysaccharide hyaluronic acid (HA) acts as lubrication throughout the body and possesses sites for both hydrogen bonding and chemical modification (Figure 2).[54] HA possesses a high degree of biocompatibility and biodegradability, ensuring parts created with HA exhibit favorable biological properties.[54,55] HA undergoes a number of reactions to introduce functionality along the polymer backbone. HA reacted at primary alcohols with methacrylic anhydride produce methacrylated HA suitable for photo-cross-linking.[56] Ouyang et al. described the functionalization of HA with adamantine (Ad) and β-cyclodextrin (CD) to facilitate enhanced supramolecular behavior via guest–host interactions.[57,58] The primary alcohol group catalyzed Ad functionality,[58] while modifying the carboxylic acid group included CD functionality.[57] Additionally, a coupling reaction through the carboxylic acid group using *N*-(3-(dimethylamino)propyl)-*N*′-ethyl-carbodiimide (EDC) yielded thiol-functionalized HA.[59] A thiol–ene reaction through thiol-HA included diaminohexane (DAH) or cucurbit[6]uril (CB[6]) into the biopolymer, which acted as guest–host supramolecular functionality facilitating the formation of hydrogels.[60,61] In addition to the inherent hydrogen bonding found in HA, the addition of functionality to either induce additional supramolecular interactions or provide chemical cross-linking to bolster HA mechanical properties provides a robust biopolymer suitable for AM.

While HA dominates polysaccharides used for AM, others such as chondroitin sulfate (CS), dextran, chitosan, sodium alginate, and gellan gum also possess favorable functionalities (Figure 2).[53] CS acts as an extracellular matrix (ECM) protein capable of withstanding compressive load and absorbing water within cartilage in the human body.[62] Its abundance of ionic groups and hydrogen bonding groups, together with sites for chemical modification, make CS an attractive choice for biologically derived structures. Abbadessa et al. described the creation of CS-methacrylate for AM through a reaction at the primary alcohol group with glycidyl methacrylate.[63]

In parallel to a partially methacrylated triblock copolymer, CS-methacrylate created synthetic cartilage tissue scaffolds.[63] CS also reacted with 2-aminoethyl methacrylate through EDC coupling to form methacrylated CS.[64] Dextran, a colloidal biopolymer, functions to resist protein adsorption and enables numerous *in vitro* characterizations of synthetic tissue scaffolds.[65] The primary alcohol on dextran reacted with hydroxyethyl methacrylate to form photocurable

DOI: 10.1021/acs.biomac.7b00671
Biomacromolecules 2017, 18, 2669–2687

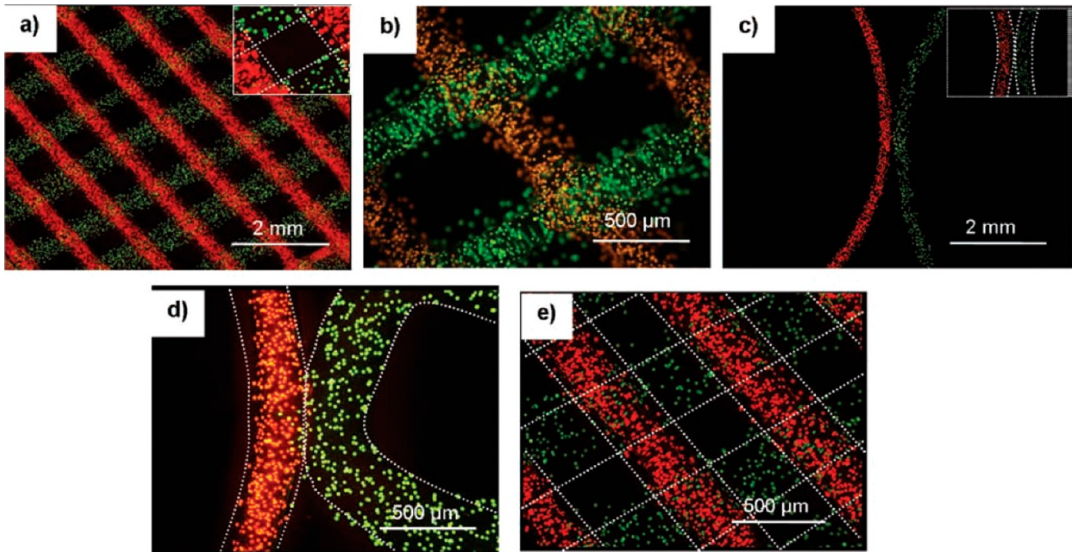

Figure 3. Material extrusion AM of poly(HPMAm-lactate)-PEG triblock copolymer generates precisely controlled deposition of polymer strands doped with fluorescent beads, including layers (a, b, e) and curves (c, d). Reprinted with permission from ref 82. Copyright 2011 WILEY-VCH Verlag GmbH & Co. KGaA, Weinheim.[82]

polymers.[66] Gellan gum, a polysaccharide commonly isolated from bacteria, possesses a number of hydroxyl groups, both primary for functionalization and secondary to serve solely as hydrogen bonding units.[67] EDC coupling through the carboxylic acid group on gellan gum afforded peptide-modified gellan gum for enhanced cell proliferation.[68] Characterization of the degree of functionality of these biopolymers provides a unique challenge due to the size and complexity of natural polymer structures.

Due to the combination of high molecular weight and supramolecular functionality, biopolymers often undergo printing in their natural state. Other polysaccharides commonly used in hydrogel formation include chitosan, which is often used in its natural form due to its intrinsic positive charge to create ionically based hydrogels.[69,70] Chitosan also reacted through acid−base chemistry to yield N,O-carboxymethyl chitosan, which results in carboxylic acid groups attached to the amine and primary alcohol.[71] Sodium alginate's native state also provided charged biopolymers capable of physical cross-linking in the presence of divalent cations, typically calcium.[72] Agarose, with a gel point below room temperature, underwent successful inkjet printing to form well-defined structures in its native state.[73] While these biopolymers often facilitate AM in their native state, their plethora of functional groups provides additional handles for chemical modifications.

Natural polymers also include polyamides generated from the polymerization of amino acids (polypeptides). The naturally occurring ECM protein collagen and its derivatives act as structural proteins and often display natural cell adhesion sequences to promote tissue generation. The arginine-glycine-aspartic acid (RGD) sequence as well as its triple helix structure make collagen an ideal candidate for the formation of tissue scaffolds. In traditional tissue engineering, collagen cross-links during the neutralization of acid-soluble collagen to form an insoluble network, suffering from significant variation and lack of control.[74] Due to these factors, along with its substantial molecular weight, collagen alone rarely permits processing through AM.[75] Instead, its derivative gelatin facilitates AM to form complex 3D structures while maintaining the biocompatibility and biodegradability benefits of collagen.[70,76,77] Commonly, reactions of methacrylic anhydride with the amine group of gelatin generated photo-cross-linkable functionality, which lent additional structural support to the printed scaffold following material extrusion AM.[76,77] Acetylation of gelatin is also accomplished at the amine group through a similar reaction.[78] Klotz et al. provided a comprehensive review of reactions with gelatin to generate 3D-printable gelatin through a variety of chemical modifications.[75] Polypeptides, while potentially offering tuned microstructure through the polymerization of different amino acids, represent only a portion of current research into biopolymer AM.

2.2. Synthetic Supramolecular Polymers. Synthetic supramolecular polymers are achieved through one of two routes: synthesis or self-assembly of a new supramolecular polymer system or modification of existing synthetic polymers. Synthetic polymers offer the ability to tune specific properties and supramolecular interactions through monomer selection or postpolymerization modifications. This control enables the selective creation of well-defined AM parts across many length scales, achieved through both printing parameters and the supramolecular chemistry employed.

2.2.1. Synthesis and Self-Assembly of Supramolecular Polymers. Synthetic chemistry facilitates precise tuning of polymeric structure, achieving control over the final printed part free from heterogeneity. Ionic interactions strongly influence hydrogel integrity, as exemplified by a zwitterionic system containing photo-cross-linkable, synthetic monomers carboxybetaine acrylamide and carboxybetaine dimethacrylate, which afforded hydrogels of varying stiffness for the preservation of human stem cells.[79] Varying ratios of acrylamide to dimethacrylate controlled modulus of gel constructs and helped direct stem cell differentiation.[79] Schultz et al. described the creation of a novel charged phosphonium monomer, which was coprinted with PEG dimethacrylate through vat photopolymerization.[8] These parts demonstrated the capability to print synthetic ionic monomers to create a supramolecular, cross-linked network.[8]

Hydrogen bonding remains one of the most prevalent and versatile form of supramolecular interactions between synthetic polymers. Free radical polymerization to form precursor copolymers of poly[(ethylene glycol methyl ether methacrylate)-*co*-*N*,*N*-dimethylacrylamide] demonstrated significant hydrogen bonding capabilities when coprinted with cellulose nanofibrils.[80] Wang et al. detailed the creation of this copolymer to specifically eliminate ionic interactions, which could cause premature gelation, and instead designed the copolymer to tailor interactions with cellulose through hydrogen bonding.[80] Acrylamide monomers containing Ad and cucurbit[7]uril (CB[7]) polymerized through free radical polymerization formed cross-linked hydrogels upon mixing.[81] Controlled free radical polymerization yielded poly(*N*-(2-hydroxypropyl) methacrylamide lactate-*co*-PEG) (Poly(HPMAm-lactate)-PEG) triblock copolymers with controlled hydrophilic/hydrophobic interactions.[82] The thermal behavior of poly(HPMAm-lactate) blocks afforded dynamic hydrogels capable of supramolecular interactions controlled through temperature, which precisely tuned the deposition of fluorescent beads (Figure 3).[82]

DOI: 10.1021/acs.biomac.7b00671
Biomacromolecules 2017, 18, 2669−2687

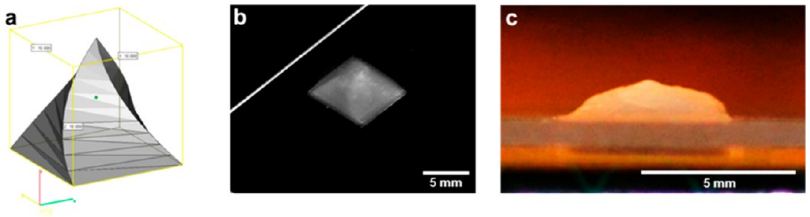

Figure 4. Inkjet printing of modified PCL from modeling (a) reveals structural integrity (b) and merging of layers (c) to produce a homogeneous pyramid. Reprinted with permission from ref 89. Copyright 2016 American Chemical Society.[89]

Step-growth polymerization to form polyurethanes that possess water solubility and biodegradability utilized a multistep procedure ending with chain extension of polycaprolactone (PCL) or poly(ether-*b*-amide) (PEBA)-based diisocyanates with ethylene diamine to form high molecular weight polymers.[83] These multifaceted hydrogen-bonding polymers form complex tissue scaffolds for material extrusion AM.[83,84] Release of chondrogenic growth factors and mesenchymal stem cell proliferation and differentiation furthered the use of AM with biodegradable polyurethanes for tissue engineering.[84]

Supramolecular interactions also promoted the self-assembly of synthetic small molecules to form complex microstructures. Amphiphilic pyrene pyridinium and 2,4,7-trinitrofluorenone were combined to create hydrogels through charge-transfer supramolecular interactions.[85] These injectable small molecules formed defined hydrogels, which also underwent self-recovery upon strain, highlighting the strength of these supramolecular interactions.[85] Wei et al. detailed the synthesis of a hydrogel, which underwent self-assembly to form a partially gelled intermediate through supramolecular interactions of amino acid-modified acrylic acid.[86] Following initial gel formation, cross-linking achieved through enzymatic polymerization formed an interpenetrating network resulting in superior mechanical properties than either gel alone.[86,87] This research exemplifies the need for incorporating supramolecular interactions into commonly utilized AM technologies to enhance or tune properties of the final part.

In each of these cases, new monomer synthesis enabled the creation of novel supramolecular polymers or fueled direct AM with a functional copolymer. As the field of supramolecular chemistry moves toward AM of isotropic parts, both new monomers and creative microstructures of commercially available monomers will enable precise control of structure, both at the molecular and printing scales.

2.2.2. Modifications of Existing Synthetic Polymers. Extensive research revealed classes of polymers suitable for use as tissue scaffolds, including PEG and PCL, each undergo chemical modifications to lend 3D-printable and supramolecular functionality. High molecular weight PCL lacks printability by methods other than extrusion AM, but offers favorable biomechanical properties.[88] To create PCL amenable to other AM techniques, modification of low molecular weight diols with supramolecular functionality is necessary.[89] Hart et al. discussed the modification of PCL diols with a multitude of hydrogen bonding and π-stacking moieties through 2,4-toluene diisocyanate end-capping reactions.[89] The inclusion of these groups at relatively low concentrations led to the formation of supramolecular networks that exhibited shear thinning behavior and successful inkjet printing, a property commonly observed in high molecular weight polymers (Figure 4).[89] Synthetic groups tailored to contain multiple hydrogen bonding groups facilitated supramolecular interactions, such as 2-ureido-4[1H]-pyrimidinone (UPy) developed by Meijer et al., which found use in a wide variety of polymeric systems.[1,52,90] UPy engaged in quadruple hydrogen-bonding and facilitated self-assembly polymers, exhibited through end-capping reactions with PCL and peptides.[90]

PEG possesses a significant portion of tissue engineered scaffolds due to its well-characterized biocompatibility and ease-of-use.[91] While the vast majority of PEG utilized for additive manufacturing exists as PEG-acrylate, the primary alcohol end-groups provided a facile route to introduce supramolecular functionality. Hydrogen bonding urethane-containing groups added to PEG diol ends through reactions with diisocyanate HMDI yielded photo-cross-linkable oligomers.[92]

3. ADDITIVE MANUFACTURING OF SUPRAMOLECULAR POLYMERS

AM consists of many forms to successfully manufacture tissue scaffolds, including material extrusion, vat photopolymerization, inkjet printing, and bioprinting.[93] Each printing technique offers its own advantages and disadvantages as well as required polymer properties to successfully employ the printing technique. Thus, various design considerations must be taken into account when developing new supramolecular polymers, which is heavily dependent on the printing technique employed. Previous literature has summarized the need for various printing methods and justifications for selection in detail.[94−100]

Bioprinting refers to cell-laden polymer solutions or resins, which subsequently undergo the printing process. Many scaffolds, however, undergo the printing process before introducing cells, eliminating additional printing parameters which could compromise the printability of the supramolecular polymer. Sterilization of tissue scaffolds occurs either before the printing process to yield sterile scaffolds directly or following scaffold formation through traditional sterilization of the preformed tissue scaffold. Sterilization adds another hidden parameter to AM tissue scaffolds, which potentially affects the structural integrity, anisotropy, and resolution of manufactured parts.

3.1. Material Extrusion Additive Manufacturing. Material extrusion AM traditionally relies on thermoplastics printed from either a hot-melt or filament. Extensive research refined the printing parameters, temperatures, and geometries for printing common polymers such as acrylonitrile-butadiene-styrene (ABS) and polycarbonate. In recent years, however, material extrusion AM of biocompatible polymers such as PCL and natural biopolymers proved valuable to the creation of tissue scaffolds for personalized medicine.

Supramolecular polymers are prevalent in material extrusion AM, both in fused filament formation and direct-write systems, largely due to the abundance of extrudable natural polymers and their inherent supramolecular functionality. Naturally occurring polymers often print with a combination of material extrusion and photo-cross-linking, as they generally have sufficient molecular weight, and thus viscosity, to achieve part fidelity upon extrusion but require photo-cross-linking to lend additional mechanical support.

3.1.1. Natural Polymers. HA features prominently for AM of tissue scaffolds, with a variety of chemical modifications resulting in the successful creation of hydrogels. HA successfully underwent modification with supramolecular functionality or photo-cross-linking groups for use in extrusion AM as described above. Highley et al. detailed the extrusion of Ad, CD and methacrylated HA, to form supramolecular bonds after exiting the nozzle.[57,58] Following successful extrusion,

DOI: 10.1021/acs.biomac.7b00671
Biomacromolecules 2017, 18, 2669−2687

photo-cross-linking the methacrylates further bolstered the hydrogel, yielding self-supporting structures.[57,58] Furthermore, microchannels within the part, created through the removal of excess un-cross-linked HA, utilized CD solutions.[58] Use of fibroblast cells confirmed functional structures capable of sustaining life, which drove future research to include the introduction of mesenchymal stem cells.[58]

Gellan gum, with combinations of other macromolecules or modified with methacrylates, encouraged successful material extrusion AM.[101−103] When modified with RGD, gellan gum formed complex layered structures without further modification or coextrusion.[68] Gellan gum and alginate supported mesenchymal stem cell proliferation and differentiation following material extrusion AM.[101] Cell seeding with human mesenchymal stem cells confirmed the improvement in cellular attachment and proliferation on composite hydrogels as compared to alginate alone.[101] Modified chitosan, coextruded with polyphosphates and alginate, formed durable hydrogels capable of additional cross-linking with calcium.[71] Osteogenic cells seeded onto these scaffolds revealed biomineralization, suggesting a strong correlation between combination hydrogels and mineralization potential.[71]

Due to their high molecular weight and native supramolecular functionality, material extrusion AM of biopolymers in their natural state catalyzes the formation of distinct tissue scaffolds. Material extrusion of alginate created hydrogels with well-defined structure.[104] Liu et al. evaluated the effect of varying deposition parameters on the resulting ionically cross-linked hydrogel, providing valuable metrics for future study.[104] Gelatin, also extruded in its native form, created 3D structures with homogeneous polymer distribution throughout, generating high-fidelity parts.[105] Gelatin also extruded with silk to create stable, implantable hydrogels suitable for soft tissue reconstruction of precisely controlled features imaged with CT scans of patient defects.[106] Alginate and gellan gum in their natural state provided hydrogels capable of releasing a number of growth factors to stimulate endothelial cell proliferation for the correction of bone defects.[107] Collagen coextruded with hydroxyapatite to sustain bone marrow stromal cell viability when seeded after printing.[108] The 3D tissue scaffold induced cell differentiation and new bone formation following implantation into a rabbit.[108] Collagen also sustained and induced proliferation of mesenchymal stromal cells following material extrusion into complex tissue scaffolds.[109] These combinations of natural polymers commonly exist as either blends or core/shell filaments, as seen in Figure 5.[110] A novel deposition system afforded core/shell scaffold materials to capitalize on the benefits of each biopolymer for the creation of precise tissue scaffolds with tunable modulus.[110]

Tissue scaffolds remain a vital portion of biological applications of 3D printing, however printing controlled release tablets to precisely tune drug therapies emerged as new materials for 3D printing continue to develop. Hydroxypropyl methylcellulose (HPMC) extruded with active ingredients formed controlled-release tablets.[111] A paste of HPMC with the drug guaifenesin produced bilayer tablets capable of controlled release.[111] This emerging aspect of natural polymer material extrusion, along with the traditional formation of tissue scaffolds, holds tremendous promise for creation of complex AM parts.

3.1.2. Synthetic Polymers. Synthetic polymers offer substantial control over supramolecular interactions and their distribution along the polymer backbone. However, introducing

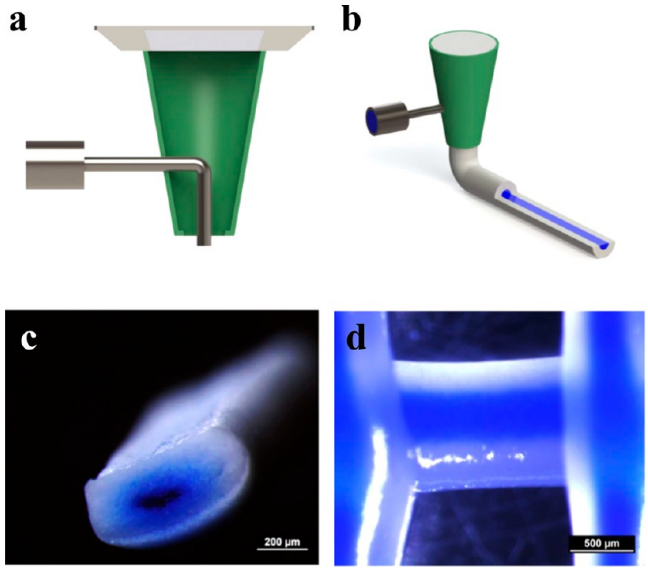

Figure 5. Schematic representation of core−shell biopolymer deposition (a−b) with dye-loaded filament (c−d) maintaining core−shell structure following material extrusion. Adapted with permission from ref 110. Copyright 2016 IOP Publishing Ltd. http://iopscience.iop.org/article/10.1088/1758-5090/8/4/045001/meta.[110]

cells onto these novel polymers generates additional unknown factors, such as biocompatibility, cell attachment, and potential cell differentiation. Furthermore, cells must produce ECM rather than embed themselves into an extruded ECM, offering the benefit of a naturally occurring ECM with the drawback of substantial time required to generate complex tissues (Figure 6).

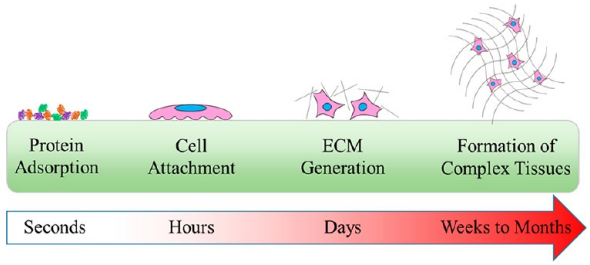

Figure 6. Time-scale of interactions with tissue scaffolds. Upon initial immersion into biological media, proteins undergo adsorption to the surface, both specific and nonspecific.[117] Cell attachment to the polymer progresses over the course of hours. ECM generation begins within days and progresses to the formation of complex tissues over the course of weeks.[118]

Material extrusion AM of the commercial ion-containing polymer Eudragrit afforded a wide array of parts for drug delivery applications. Ethyl acrylate, methyl methacrylate, and trimethylammonioethyl methacrylate chloride copolymerized to form Eudagrit, which possessed a T_g of 63 °C. Pietrzak et al. detailed the creation of drug-doped filament and successful extrusion AM to create well-defined tablets, examining the effect of print resolution on dosing and controlled release.[112] Eudragrit also inspired use as a hot-melt extruded transdermal patch,[113] extruded granules,[114,115] and floating pellets,[116] driving future use to control pharmaceutical release.

The high degree of hydrogen bonding inherent to the urethane bond catalyzes polyurethane use in synthetic supra-

DOI: 10.1021/acs.biomac.7b00671
Biomacromolecules 2017, 18, 2669−2687

molecular polymers.[83] Polyurethane resins successfully extruded to create complex parts with favorable surface roughness.[119] The use of shape-memory polymers resulted in parts for robotic mechanisms, resulting in a gripper suitable for grasping fine objects which operates through transition through the polymer's glass transition temperature.[119] PCL-based polyurethane tissue scaffolds provided support for mesenchymal stem cell proliferation and differentiation, as well as released growth factors to induce new cartilage formation.[83,84]

Tuned supramolecular interactions provide a mechanically robust material compared to polymers with nonspecific supramolecular interactions. Chen et al. detailed the coextrusion of polyacrylamides containing CB[7] and Ad to form guest−host interactions between polymer chains.[81] Upon mixing, a strong hydrogel formed that exhibited bulk properties and compressive hysteresis.[81] Polyion complexes composed of poly(sodium *p*-styrenesulfonate) (anionic) and poly(3-(methacryloylamino)propyl-trimethylammonium chloride) (cationic), extruded in the presence of saline, demonstrated the power of ionic interactions to form stiff hydrogels.[120] With the diffusion of counterions out of the printed hydrogel, the polyelectrolytes formed a tough network based solely on supramolecular interactions.[120] While relations between extruded synthetic polymers and biologics are in their infancy, the vast array of potential new polymers for material extrusion AM make it an attractive choice for future investigations.

3.1.3. Polymer Blends. Blends of synthetic and natural polymers often coextrude to exert control over polymer structure inherent to synthetic polymers, while harnessing the naturally occurring supramolecular functionality and biocompatibility present on biopolymers. Khaled et al. detailed the material extrusion AM of a hydroxyl methylcellulose-poly(acrylic acid) hydrogel for sustained release drug tablets which exhibited enhanced mechanical properties compared to commercially available products.[111] The interactions between the synthetic and natural polymer, tuned through their weight ratios, revealed a low amount of poly(acrylic acid) needed to provide superior mechanical properties.[111] PEG continues to capture the majority of tissue scaffold generation due to its biocompatibility and precedence. PEG-diacrylate coupled with gelatin, agarose, and alginate extruded into a concentrated salt solution to yield distinct scaffolds onto which myoblast cells were seeded.[121] Abbadessa et al. coprinted PEG-tetraacrylate with CS to yield well-defined, porous structures capable of sustaining chondrogenic cells for at least 6 d.[63] These hydrogels capitalize on the favorable supramolecular properties of biopolymers coupled with the well-known biocompatibility of PEG.

PCL also exhibits favorable biodegradability and biocompatibility, catalyzing its use in tissue engineered scaffolds. UPy-modified PCL and peptides coprinted to create 3D structures with significantly enhanced mechanical and biological properties as compared to either polymer individually.[90] Hydrogen bonding between the two oligomers afforded a structurally sound scaffold upon extrusion which sustained fibroblast viability.[90] Methacrylated poly(hydroxymethylglycolide-*co*-ε-caprolactone) codeposited with gelatin-methacrylate yielded strong hydrogels with both complex hydrogen bonding and covalent cross-linking.[122] These hydrogels, implanted in rats, sustained chondrocyte viability and promoted collagen production *in vivo*.

Due to its high charge density and facile cross-linking through calcium, alginate in its native form offers an extrudable biopolymer without need for chemical modification. Alginate and PEG-diacrylate coextruded to form mechanically robust hydrogels capable of self-healing, approaching properties of native hydrogel.[123] These self-healing characteristics also enabled layer interactions to form parts that approached mechanical properties of bulk material. Human mesenchymal stem cells embedded in the tissue scaffolds underwent elongation upon hydrogel straining, suggesting strong cellular attachments and the potential to differentiate cells based on elongation.[123] Alginate also extruded alongside *N,N′*-methylenebis(acrylamide) to form hydrogels cross-linked ionically by calcium chloride and covalently by UV irradiation.[124] Stress−strain behavior of extruded hydrogels tuned with varying ratios of alginate to acrylamide changed the degree of ionic associations to covalent networks to reveal idealized hydrogels.[124]

Nucleic acids are known for their extreme hydrogen bonding capabilities, highlighted through the material extrusion AM of polystyrene or polyacrylamide beads coated with complementary DNA strands.[125] These materials successfully formed well-defined 3D structures without the need for support material or solvent for printing, demonstrating the power of supramolecular interactions in structure formation.[125] Human skin cells seeded onto these colloidal gels maintained viability and exhibited proliferation and colonization within the gel, emphasizing both the mechanical and chemical properties of the resulting hydrogel.[125]

Material extrusion AM offers the ability to employ commercially available polymers and biopolymers to generate tissue scaffolds of millimeter-scale resolution without the need for extensive chemical modifications. Furthermore, the natural properties of biopolymers act in conjunction with extrusion-based AM due to their high molecular weight and high viscosity. The diversity of supramolecular polymers suitable for material extrusion AM provide a solid foundation for future innovation and tissue scaffold development.

3.2. Vat Photopolymerization. Vat photopolymerization revolves around the use of light and a photoactive polymer to create intricate 3D structures. Either a top-down or bottom-up approach coupled with a movable stage and masks or mirrors patterns a specific structure in a layer-by-layer fashion. Control of light intensity, photopolymer characteristics, and photoinitiator/photoabsorber content catalyzes the creation of fine features, which is well reviewed elsewhere. Biologically friendly photoinitiators govern biological interactions with 3D tissue scaffolds, with few water-soluble and biologically compatible photoinitiators currently in use. Vat photopolymerization affords a number of scaffolds relevant for tissue engineering due to its resolution capabilities, but lacks significant examples of supramolecular polymers.[100,126,127]

Traditional vat photopolymerization of PEG incorporated supramolecular and biodegradable functionality with the addition of depsipeptide, a derivative of L-alanine.[128] Degradation and cell viability measured with depsipepetide-PEG scaffolds revealed that mass loss and cell proliferation occurred simultaneously, indicating a hydrogel supportive of cell growth and complex tissue formation.[128] Lutrol F127, a copolymer of PEG and poly(propylene glycol), modified with dipsipeptide, also successfully printed by vat photopolymerization.[129] The inclusion of dipsivpeptide to the copolymers resulted in enhanced cell viability as compared to the copolymer alone, suggesting the importance of depsipeptide in both printing processes and maintenance of cell viability.[129] Highlighting the

DOI: 10.1021/acs.biomac.7b00671
Biomacromolecules 2017, 18, 2669−2687

diversity of PEG in tissue scaffold formation, PEG diacrylate photo-cross-linked with chitosan revealed ear-shaped tissue scaffolds with varying porosity which, upon seeding with mesenchymal stem cells, maintained high cell viability.[69]

Hydrogen bonding urethanes facilitate AM of isocyanate-free polyurethane oligomers, which accomplishes gradient structures.[130] Mouse fibroblast cells seeded onto polyurethane scaffolds exhibited high cell viability suggesting potential for future *in vivo* applications.[130] Tissue scaffolds generated with urethane diacrylate sustained bone marrow stromal cells, with enhanced proliferation and metabolic activity than their 2D counterparts, as shown in Figure 7.[131] Bone marrow stromal

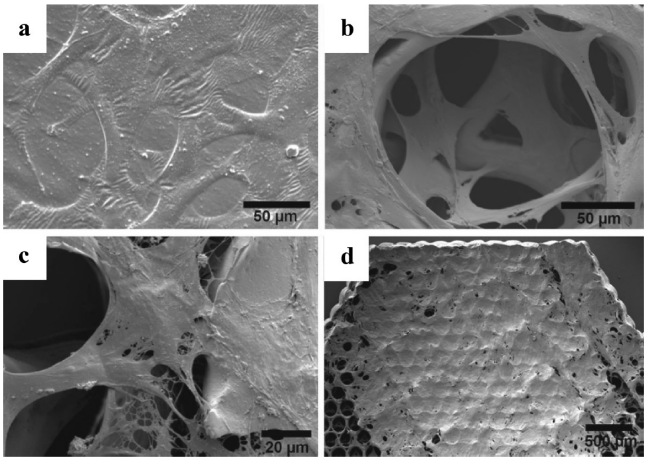

Figure 7. Bone marrow stromal cells exhibit 3D growth (a–c) and differentiation (d) upon seeding into urethane diacrylate tissue scaffolds printed with vat photopolymerization. Adapted with permission from ref 131. Copyright 2014 WILEY-VCH Verlag GmbH & Co. KGaA, Weinheim.[131]

cells spread in 3D to completely cover pores generated during vat photopolymerization, facilitating the creation of functional bone tissue.[131] Chung et al. reported modification of PEG with urethane moieties to induce hydrogen bonded, well-defined parts through vat photopolymerization.[92] Cell viability exceeded 75% for all scaffolds, with the highest viability resulting from higher molecular weight PEG oligomers.[92] End-capping reactions of polyesters also imparted hydrogen bonding to allow successful vat photopolymerization of engineered tissue scaffolds.[132] Hydrogen bonding and ionic interactions coupled through the printing of diurethanedimethacrylate, glycerol dimethacrylate, and quaternary ammonium-modified methacrylates formed semi-interpenetrating networks.[133] This system not only exhibited superior antimicrobial activity, but also provided a facile system to introduce hydrogen-bonding into the AM part.[133]

Natural polymers leverage a large portion of the vat photopolymerization printing for biological applications due to their expected cell affinities and established chemistries used to modify their complex structures. HA in particular experiences widespread use in printing cell scaffolds from vat photopolymerization.[55,134,135] Chitosan coprinted with PEG-diacrylate yielded ear-shaped scaffolds suitable for chondrocyte culturing.[69] Both high and low molecular weight charged chitosan and varied ratios of PEG-diacrylate enabled successful vat photopolymerization to form porous, complex scaffolds.[69] Supramolecular biomaterials also include deoxyribonucleic acid (DNA) and proteins, which formed 3D structures containing photo-cross-linked DNA through vat photopolymerization.[136] Bovine serum albumin, DNA, and gelatin printed both with two-photon microfabrication and vat photopolymerization to produce precise structures.[136] Photo-cross-linkable keratin hydrogels synthesized by vat photopolymerization revealed the maintenance of fibroblast viability, expanding the collection of biopolymers created with this approach.[137]

Hydrogels synthesized using water-soluble, biocompatible photoinitiators drive the future of vat photopolymerization for biologically relevant scaffolds. Pawar et al. synthesized water-soluble nanoparticles containing photoinitiator to print aqueous acrylamide solutions with high resolution when coprinted with PEG-diacrylate.[138] These scaffolds sustained cell viability and contained ∼80% water, previously unachievable due to the lack of water-soluble photoinitiators.[138] Vat photopolymerization research thrusts, both in the area of water-soluble photoinitiators and supramolecular oligomers, stimulates the generation of increasingly complex tissue scaffolds with enhanced resolution as compared to its AM counterparts.

3.3. Bioprinting. Bioprinting involves AM of a cell-laden polymer solution by either microextrusion, inkjet printing, or laser-assisted printing, which often blurs the lines between traditional AM techniques and bioprinting.[9,139] These types of printing are well reviewed elsewhere.[13] Briefly, microextrusion bioprinting revolves around the syringe deposition of cell-laden material. Inkjet involves the deposition of droplets onto a surface to create a 3D-structured object. Laser-assisted deposition utilizes a laser pulse to transfer material containing cells onto a substrate. In each of these techniques, cells undergo the printing process, necessitating a biological ink that sustains cell viability throughout the print as well as provides structural integrity suitable for a particular biological application.[140−142]

Cartilage and cartilage-forming cells (chondrocytes) often find widespread use in the field of tissue engineering due to their ease of handling and resiliency toward modified biopolymers and synthetic polymers.[143,144] Chondrocytes also induce the formation of complex ECM structures, easing characterization of healthy cell-laden tissue scaffolds.[102] Dextran-HA hydrogels formed through microextrusion and subsequent photocuring yielded semi-interpenetrating network scaffolds suitable for cartilage tissue engineering.[66] Precise control of printing parameters and hydrogel swelling evaluated for a number of hydrogel compositions all sustained chondrocyte viability.[66] Thermally sensitive poly(HPMAm-lactate)-PEG hydrogels printed in a similar fashion yielded hydrogels structured through hydrophobic interactions arising from the microstructure of the triblock copolymer.[82] Encapsulated chondrocytes maintained viability throughout the printing process to produce well-defined structures possessing precise control of cell localization.[82] Chondrocyte-laden methacrylated and acetylated gelatin solutions underwent inkjet printing to impart well-defined droplets on preformed gelatin hydrogels.[78] These inks sustained cell viability despite the degree of functionality of gelatin and varying incubation times (up to 240 min) prior to printing, indicating the ability of gelatin inks to afford complex tissue scaffolds with high cell viability.[78]

Stem cells specifically differentiate into varied daughter cells based on their chemical and physical environment. Based on the stem cell origin, differentiated cells could manifest as a wide variety of cell types, adding a layer of complexity to the printing process to prevent stem cell differentiation.[145] Supramolecular microextrusion bioprinting accomplished with PCL, atelocolla-

DOI: 10.1021/acs.biomac.7b00671
Biomacromolecules 2017, 18, 2669−2687

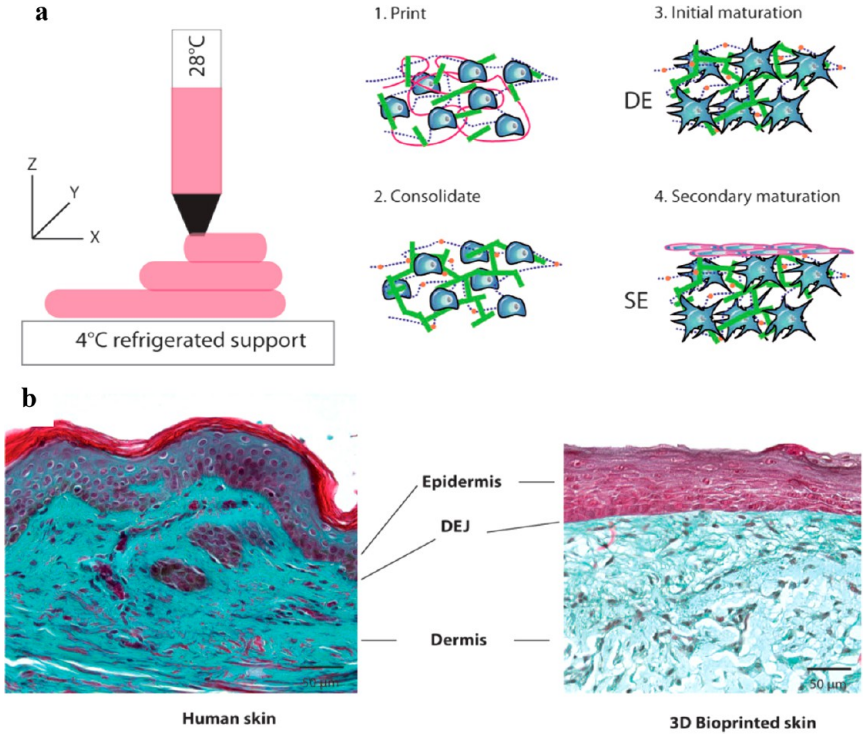

Figure 8. (a) Schematic representation of skin tissue printing, growth, and maturation upon 3D printing with natural ECM. (b) Following 26 d incubation, synthetic skin mimicked healthy human donor skin, revealing a bioprinting route to functional, synthetic skin. Adapted with permission from ref 149. Copyright 2017 WILEY-VCH Verlag GmbH & Co. KGaA, Weinheim.[149]

gen, and modified hyaluronic acid yielded 3D structured scaffolds embedded with turbinate-derived mesenchymal stromal cells for osteochondral tissue regeneration.[61] These multimaterial scaffolds successfully promoted cartilage generation in a rabbit knee joint and paved the way for future multimaterial printing without the need for harmful cross-linking agents.[61]

Inkjet bioprinting with mesenchymal stem cell-laden methacrylated gelatin accomplished by Gurkan et al. formed anisotropic fibrocartilage.[146] To closely mimic the transition between tendon and bone, gelatin droplets containing cells and one of two growth factors deposited side-by-side to produce a complex tissue geometry containing a biochemical gradient suitable for personalized medicine and new drug therapy testing.[146] Supramolecular interactions derived from peptides enhanced both function and cell viability of inkjet-printed PEG-diacrylate to form mesenchymal stem cell-laden hydrogels.[147] Gao et al. described stem cell differentiation, subsequent production of cartilage, and detailed the ability of bioprinting to produce homogeneous, cell-laden scaffolds.[147] While these examples highlight the use of bioprinting to generate nonvascular tissues, the use of stem cells to derive differentiated tissues with specific phenotypes will drive future work in synthetic tissue engineering.

Multimaterial and multicell bioprinting carries the ability to achieve complex scaffolds that closely mimic native tissues and organs. Gelatin served as an effective biopolymer for bioink AM, especially when mixed with other natural (collagen, fibrinogen) or synthetic (PEG amine) macromolecules to enhance physical properties of the resulting 3D printed part.[77] Multimaterial printing controlled both the bioactivity of human dermal fibroblasts as well as the structural characteristics of the 3D printed part to allow for diverse tissue scaffold properties as a function of polymer blend.[77] Complex skin tissue formed through inkjet bioprinting of fibroblast and keratinocyte-containing bioinks composed of alginate and EDTA.[148] Precise control of layered structures varying between fibroblast and keratinocyte-laden inks successfully afforded functional skin tissue.[148] Pourchet et al. detailed the creation of functional human skin that mimics healthy donor tissue following culture for 26 d, as shown in Figure 8.[149] Engineering synthetic neurons remains the pinnacle of avascular tissue engineering due to the complexity and sensitivity of neuronal cells. Lozano et al. detailed the microextrusion bioprinting of modified gellan gum with and without cortical neurons, producing a layered structure capable of maintaining cell viability.[68] Interestingly, the neurons remodeled and infiltrated the neighboring layers, suggesting not only an enhancement of cell activity but also the reversible ionic physical cross-links.[68] While avascular tissue engineering limits the complexity needed in scaffolds, the cell types and potential supramolecular polymer utilization requires precise control for the creation of biologically mimicking scaffolds.

Scaffolds of complex metabolic function capable of examining drug discovery and disease states require printing of complex cells types and the subsequent generation of characteristic phenotypes.[150] Gelatin, alginate, and fibronigen mixtures microextruded with adipose-derived cells yielded scaffolds with high porosity capable of supporting cell viability.[151] After introducing pancreatic islets to the scaffolds, characterization of insulin release rate as a function of glucose concentration afforded a complex tissue scaffold suitable for disease examination and drug discovery (Figure 9).[151] Gelatin methacrylate printed via microextrusion followed by UV irradiation afforded porous tissue scaffolds laden with hepatocytes for synthetic liver tissue.[152]

DOI: 10.1021/acs.biomac.7b00671
Biomacromolecules 2017, 18, 2669−2687

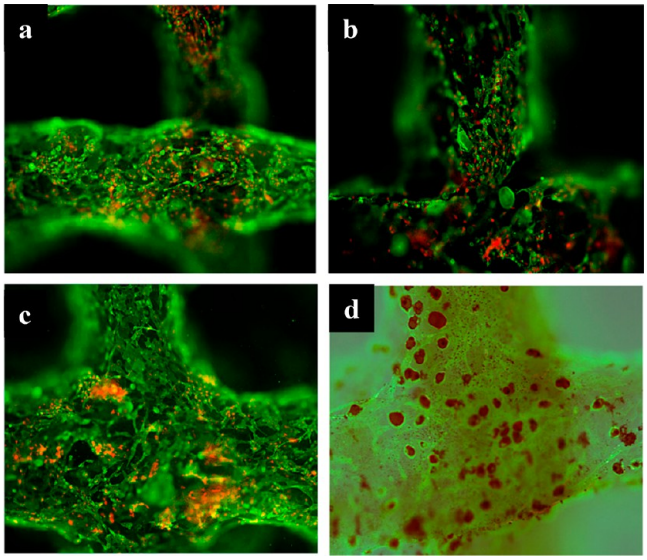

Figure 9. Adipocyte stem cell and endothelial cell bioprinting retained viability immediately following printing (green: CD34+, red: PI; a–b). Maturation of endothelial cells (c, green: CD31+, red: PI) cultured with epidermal growth factor. Adipocytes matured following treatment with insulin, 3-isobutyl-1-methylxanthine (IBMX), and dexamethasone (d, green: CD31+, red: Oil red O). Adapted from ref 151. Copyright 2010, with permission from Elsevier.[151]

Localization of the cells and the effect of nozzle types probed cell viability and hydrogel fidelity, forging the way for future studies to examine drug metabolism.[152] Complex biological tissues generated through microextrusion bioprinting to yield renal proximal tubules results in the accomplishment of biologically active renal structures.[153] Casting fibroblast-laden gelatin and fibrinogen ECM along with microextrusion of sacrificial Pluronic F127 formed complex tubule structures.[153] Perfusion with renal cells yielded a polarized epithelium mimicking natural renal structures, vital to the development of *in vitro* models to evaluate drug meatbolism.[153] While significant research revealed the generation of metabolically active tissue *in vitro*, the full utilization of synthetic tissue scaffolds for drug metabolism and disease characterization remain unexplored.

Generating vascularized tissues adds additional complications to the printing process, but affords scaffolds with increasing complexity to better mimic native tissues.[154] Skardal et al. discussed the ability of thiolated-HA and PEG of varying topology to form hydrogels and successfully microextrude cell-containing filaments.[59] Following deposition of high-viscosity filaments of HA-PEG and agarose into vessel-containing hydrogels, cellular activity remained for up to 4 weeks.[59] Furthermore, harnessing base cross-linking (NaOH) to form hydrogels prior to microextrusion bioprinting eliminated the use of harmful UV radiation and photoinitiator.[59] Laser-assisted transfer of cell-laden droplets to form complex vessel-like structures yielded high-density tissue scaffolds, which required low concentrations of alginate to produce successful prints.[155] A high concentration of cells (6×10^7 cells/mL) printed onto a fibrinogen gel substrate facilitated well-defined areas of cells of high density and viability.[155] Even the high density of cells printed in this system required the addition of small amounts of supramolecular alginate to form well-defined structures. Vascularized liver tissue, involving AM of hepatocytes and endothelial cells together, drives the generation of functional, engineered tissue for liver regeneration.[156] The inclusion of fibroblasts into the tissue scaffold proved essential for albumin secretion and urea production, facilitating future design of multicell tissue scaffolds for biomimetic tissues.[156] The generation of vascularized tissues stimulates additional complexity for organ regeneration and tissue regeneration, many aspects of which remain unexplored.

The most complex of all vascularized tissues include the heart, lungs, and cardiovascular systems, which require every type of cell from muscle to endothelial to generate functional organs. Gelatin and alginate biopolymers laden with aortic valve

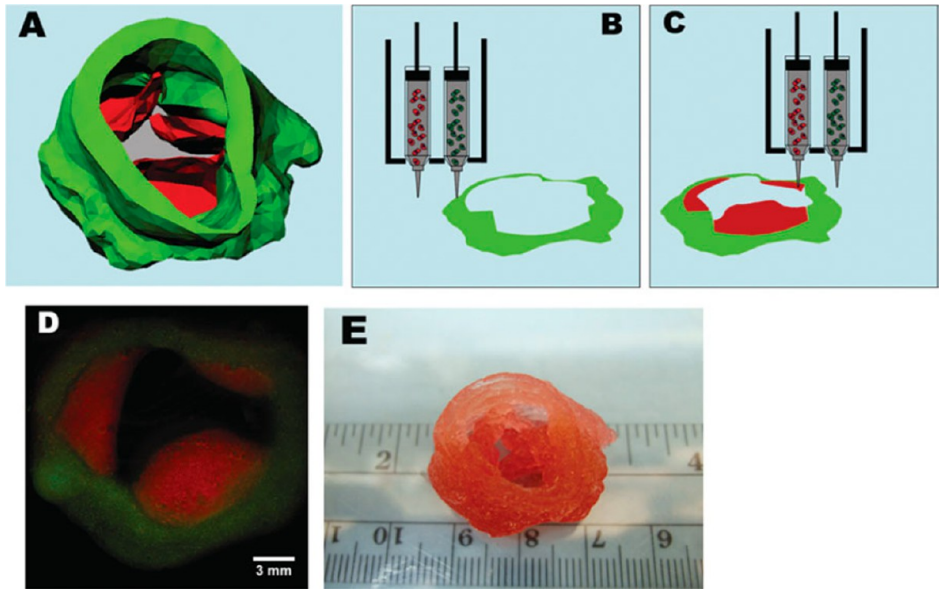

Figure 10. Aortic valve conduit bioprinting from micro-CT image (A) with both aortic valve root cells (B) and leaflet cells (C). (D, E) Fluorescence imaging revealed maintenance of conduit structure, with overall structure size mimicking that of native tissue. Reproduced with permission from ref 157. Copyright 2012 WILEY PERIODICALS, INC.[157]

DOI: 10.1021/acs.biomac.7b00671
Biomacromolecules 2017, 18, 2669–2687

Table 1. Bioprinting Affords Complex Tissue Generation Utilizing Both Common Cell Types and Increasingly Complex Cells

Supramolecular Polymers for 3D Bioprinting				
Cell Type	Printing Type	Polymer Base	Cell Concentration	References
Structural Tissues				
Skin (Fibroblasts, Epidermal)	Microextrusion	Gelatin, PEG	2×10^6	77
		Agarose, PEG, HA	2.5×10^7	59
		PEG, amino acid-acrylic acid		86,87
		Gelatin, Alginate, Fibrinogen	1×10^6	149
		Fibrinogen	7×10^4, 6×10^6	160
		Gelatin	5×10^6	161
		Gelatin, Alginate		162
	Inkjet	Alginate, EDTA blood plasma	3.33×10^7	148
		Alginate, Gelatin	1×10^6	163
Chondrocytes	Microextrusion	Poly(HPMAm-lactate)-PEG	5×10^6	82
		HA, dextran	5×10^6	66
		Gelatin, Gellan Gum	$(1-2) \times 10^7$	102
		HA-poly(NIPAAM)	6×10^6	164
		Polyethylenimine, Alginate	5×10^6	165
		Fibrinogen, Gelatin, HA	4×10^7	166
		Alginate, PCL	1×10^6	167
		HA, CS, Poly(HPMAm-lactate)-PEG	$(1.5-2) \times 10^7$	168
	Inkjet	Gelatin	1×10^6	78
Stem Cells				
Mesenchymal Stem Cells	Inkjet	Gelatin	1×10^6	146
		PEG, Polypeptide	6×10^6	147
	Microextrusion	HA	5×10^6	58
		Gelatin	5×10^5	169
			5×10^6	161
		Collagen, Gelatin		170
		Fibrinogen, Gelatin	$(0.1-10) \times 10^6$	171
		Collagen, Alginate, Gelatin	2×10^6	172
		Gelatin, HA, CS	1.5×10^7	64
		Gelatin, Alginate, Chitosan	2×10^6	173
		Silk Fibroin, Gelatin	$(2-5) \times 10^6$	174
	Vat Photopolymerization	Gelatin	5×10^6	175
Embryonic Stem Cells	Microextrusion	Gelatin, Alginate	1×10^6	176
Adipose Stem Cells	Microextrusion	Gelatin, Alginate, Fibrinogen	3×10^7	151
			1×10^6	177
		Alginate	1×10^6	140
		Alginate, Gelatin	3×10^6	178
		Collagen	1×10^6	179
Glioma Stem Cell	Microextrusion	Fibrinogen, Gelatin, Alginate	5×10^5	180
Amniotic Fluid-Derived Stem Cells	Microextrusion	Gelatin, Fibrinogen, HA	5×10^6	166
Avascular Tissues				
Neuron	Microextrusion	Gellan Gum	1×10^6	68
		Fibrinogen, HA	2×10^5	181
		Alginate	5×10^5	182
		Agarose, Alginate, Chitosan	1×10^7	183
Myoblast	Microextrusion	Fibrinogen, Gelatin, HA	3×10^6	166
Anterior Pituitary	Inkjet	Polypeptide, DNA		184
Metabolic Tissues				
Kidney	Microextrusion	Gelatin, PEO	5×10^6	185
		Gelatin, Alginate	2×10^6	186
Urethra	Inkjet	Fibrinogen, Gelatin, HA	1×10^7	187
Hepatocytes	Microextrusion	Gelatin	1.5×10^6	152
		Collagen	$(0.2-1) \times 10^6$	156
		Gelatin, Alginate, Fibrinogen	1×10^7	177
Vascular Tissues				
Endothelial Cells	Laser-assisted	Alginate, Matrigel	5×10^7	155
	Microextrusion	Gelatin, PEG	5×10^6	185
		Fibrinogen	2×10^5	188
		Collagen	2×10^5	156

DOI: 10.1021/acs.biomac.7b00671
Biomacromolecules 2017, 18, 2669−2687

Table 1. continued

Supramolecular Polymers for 3D Bioprinting				
Cell Type	Printing Type	Polymer Base	Cell Concentration	References
		Alginate, Gelatin	5×10^5	110
Aortic Valve	Microextrusion	Gelatin, Alginate	2×10^6	157
Cardiac Cells	Microextrusion	Gelatin, HA	3×10^7	189
Lung Fibroblast	Microextrusion	Collagen	$(6–7.5) \times 10^5$	156

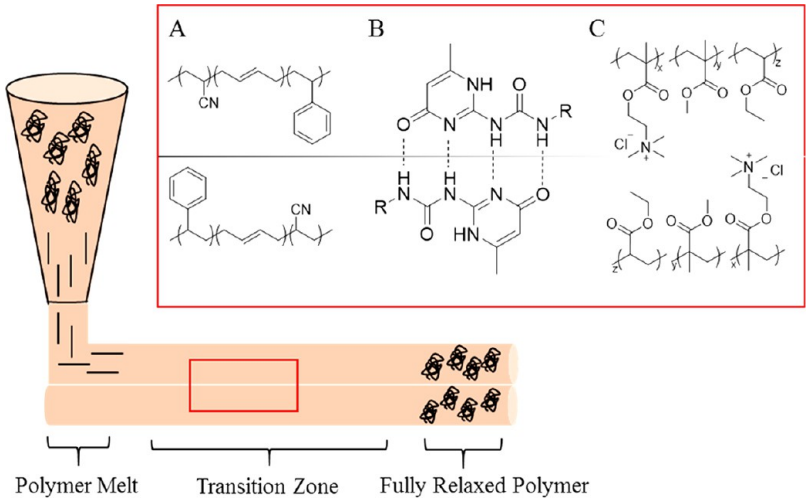

Figure 11. Effect of supramolecular polymers on anisotropy depends on the type of interaction that can occur between layers. Extrudable polymers with no supramolecular interactions, such as ABS (A) do not interact across the layers. Hydrogen bonding (B) or ionic associating (C) polymers have the ability to interact across boundaries to improve interfacial adhesion.

interstitial and smooth muscle cells afforded a complex *in vitro* model of the aortic valve.[157] Microextrusion bioprinting of these two cell types into specifically patterned regions of an aortic valve model resulted in expression of biomarkers in location-specific regions of the scaffold, as seen in Figure 10.[157] Similar scaffolds synthesized with PEG-diacrylate and alginate also yielded sophisticated aortic valve structures.[158]

Bioprinting with complex cell types to form complex scaffolds closely mimicked native biological tissue and afforded high-fidelity models to examine normal and disease-state tissues.

Bioprinting necessitates the maintenance of cell viability throughout the printing process, which introduces a complex factor to successful AM. Factors such as time of print, cell concentration, oxygen diffusion, and temperature affect both the printing process as well as the viability of the cell.[142,159] As an example, cell viability is maintained for longer times at reduced temperature, but the viscosity of cell-laden polymer solutions increases at lower temperatures, potentially hindering the printing process.[42,159] The inclusion of these additional parameters makes printing challenging, but the resulting homogeneous tissue scaffold avoids many problems faced in traditional AM of tissue scaffolds, such as cell gradients and diffusion-limited cell seeding.[142] A number of synthetic and natural polymers with their cellular counterparts exist currently (Table 1), providing a platform for future complex tissue generation through bioprinting.

4. EFFECT OF SUPRAMOLECULAR POLYMERS ON ANISOTROPY

Improving anisotropy drives supramolecular AM research, which stems from a desire to create isotropic parts for final use (Figure 11). AM without supramolecular interactions generates distinct layers with a defined interface, often the weak point in the part. One method to aid in achieving material isotropy revolves around forming interpenetrating networks, where multiple supramolecular interactions or a combination of supramolecular interactions and chemical cross-linking act in parallel to form stiff networks. Wei et al. explored this idea through agar, polyacrylamide, and alginate in concert to form tough hydrogels.[190] Initially, the AM structure demanded hydrogen bonding interactions prevalent in the agar, followed by chemical cross-linking of the acrylamide monomers to form polyacrylamide networks. Furthermore, soaking the hydrogel in calcium chloride solution induced physical cross-linking of the alginate through electrostatic interactions.[190] Following ink-based printing and subsequent photo-cross-linking, Abbadessa et al. revealed an enhancement of mechanical properties upon the inclusion of both CS-methacrylate and triblock copolymer together, suggesting the presence of an interpenetrating network.[63]

Nature perfected the use supramolecular interactions to form complex structures that have both programmed anisotropy and isotropy specific to tissue types. Harnessing the power of nature, supramolecular interactions due to complementary DNA strands mended hydrogel layers in well-defined tissue scaffolds generated from inkjet bioprinting.[184] The use of polypeptides and DNA forms isotropic hydrogels with suitable mechanical integrity to sustain cell viability.[184] Combinations of natural polymers to form polyelectrolyte hydrogel scaffolds also approach properties of bulk materials. Gelatin and chitosan combined to form extrudable polyelectrolyte hydrogels capable of sustaining skin fibroblast viability, interacting between layers to form a homogeneous scaffold.[70]

DOI: 10.1021/acs.biomac.7b00671
Biomacromolecules 2017, 18, 2669–2687

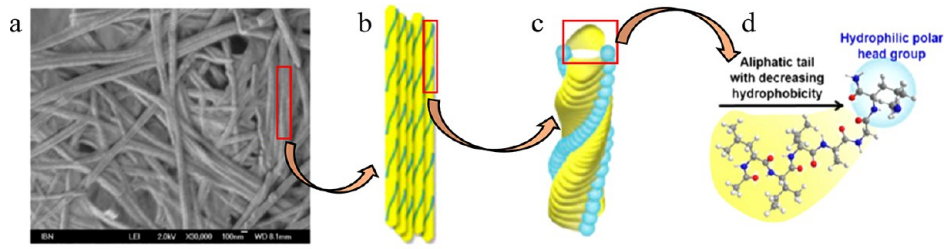

Figure 12. Hierarchical printing of peptide-based scaffolds. Scaffold structure (a) showing fibers which are composed of many β-sheets (b). β-sheets are then composed of a number of α-helices (c). α-helices are formed from short peptide sequences (d) Designed for self-assembly Adapted with permission from ref 196. Copyright 2015 American Chemical Society.[196]

Zhu et al. described polyion hydrogels which approach tensile properties of the bulk material, suggesting the power of ionic interactions to maintain structure of the hydrogel.[120] Furthermore, these polyion complexes exhibited hysteresis, highlighting the polymers' ability to reform ionic interactions after an applied load.[120] Additionally, this self-healing behavior along with comparable mechanical properties suggested isotropic behavior while offering the ability to precisely define 3D structure. The introduction of water into printed structures also imparts significant mobility to polymer chains, aiding in the formation of supramolecular interactions across layers.

5. PRINTING HIERARCHICAL STRUCTURES

Biological tissues possess well-characterized hierarchy, with many built-in layers of structure on the molecular, cell, tissue, and organ level to create functional materials.[19,52,191] The role of designing hierarchical structures for improved mechanical properties as compared to bulk materials currently revolutionizes AM and its role in both biomedical materials and structural materials.[192] Currently, hierarchy imparted onto microfluidic structures printed with PEG diacrylate yielded high-fidelity parts that exhibit fluid mixing.[175] Mimicking the hierarchy of nature provides a structure with the capability to recreate tissues for use in biomedical applications such as organ replacement, drug discovery and delivery, and structural support materials.[193,194]

Polyaniline demonstrated the potential to form these hierarchical structures through its cross-linked sheets. Dou et al. detailed the cross-linking of polyaniline with amino trimethylene phosphonic acid (ATMP) which acted to hold sheets of polyaniline in place during the extrusion AM process.[195] Furthermore, the structures produced were porous, which added a third level of complexity to the system, generating structure on the molecular, macromolecular, and feature scale.[195]

Nature is unmatched in the creation of hierarchical structures. Harnessing natural supramolecular materials to generate complex features starts to probe structures that closely mimic tissues and organs. Harnessing the ability of peptides to self-assemble into sheets and filaments, scaffolds with hierarchical structure effectively extruded to create both droplets and sheets (Figure 12).[196] The tiered nature of these scaffolds successfully cultured a variety of stem cell types as well as complex intestinal cells, highlighting the importance of hierarchical structures to *in vitro* cell and tissue viability.[196] As tissue engineering moves toward more complex synthetic scaffolds, the introduction of hierarchical structure will provide biologically robust hydrogels capable of mimicking complex natural tissues. With more biologically sound synthetic hydrogels, the fields of synthetic organ replacement and disease characterization will progress rapidly.

6. CONCLUSIONS AND FUTURE PERSPECTIVES

Supramolecular polymers remain an emerging field of research, both in the creation of novel materials and the development of biologically relevant scaffolds. Traditional tissue scaffolds suffer either from well-defined structure lacking fine features detectable by cells or supramolecular interactions that fail to provide well-defined structures. The combination of AM and supramolecular chemistry has the potential to develop hierarchical structures with levels of order spanning the entire sensing breadth of cells and creating synthetic tissues capable of mimicking native human tissues.

Achieving the final desired properties with supramolecular structures and AM remains challenging and represents an exciting new direction in biological constructs. Utilizing the self-assembly of supramolecular polymers to impart anisotropic hierarchical structures relies on predictable polymer chain dynamics and organization of the polymer morphology during processing. Understanding the role of the AM process on the resulting self-assembled structure is critical to provide guiding structure−property-processing relationships. This fundamental understanding, which remains at its infancy, will drive further innovation and breakthroughs with fabricating full organs or tissues.

Imparting mechanical property or surface gradients across tissue engineered scaffolds remains an attractive avenue to mimic native tissue. This is achieved through controlling the AM processing parameters, the design of the scaffold, or the self-assembly/hierarchical evolution of supramolecular polymers once printed. Combining the advantages of all three offers the greatest opportunity for developing a construct with the required mechanical, biological, and chemical properties to serve as a viable scaffold/tissue replacement. Thus, new natural and synthetic polymers must be designed to account for the property requirements for both AM and a hierarchical tissue scaffold. Also, combining synthetic and natural polymers offers a means to tune scaffold properties (synthetic polymer) as well as maintain biocompatibility and the inherent ability to adhere, differentiate, and proliferate cells (natural polymer).

Eventually, researchers must also further consider the targeted tissue/organ to be replaced. Currently, most research focuses on controlling porosity/architecture, evaluating new polymers, and analyzing cellular interactions with the scaffold. The overarching goal of tissue engineering for replacing full organs demands larger constructs with similar size, shape, and porosity. These properties must be evaluated to offer insight into better design processing techniques and chemistry to replicate the full target. Conquering these problems will drive

DOI: 10.1021/acs.biomac.7b00671
Biomacromolecules 2017, 18, 2669−2687

the future of tissue engineering research and translation to the creation of synthetically grown organs suitable for transplant into humans.

AUTHOR INFORMATION

Corresponding Author

*E-mail: telong@vt.edu. Telephone: (540) 231-2480. Fax: (540) 231-8517.

ORCID

Ryan J. Mondschein: 0000-0002-4960-0387

Timothy E. Long: 0000-0001-9515-5491

Notes

The authors declare no competing financial interest.

ABBREVIATIONS

AM, additive manufacturing; T_g, glass transition temperature; NMR, nuclear magnetic resonance spectroscopy; FTIR, Fourier transform infrared spectroscopy; PEG, poly(ethylene glycol); HA, hyaluronic acid; Ad, adamantine; CD, β-cyclodextrin; EDC, *N*-3-dimethyl(aminopropyl)-*N*′-ethylcabrodiimide; DAH, diaminohexane; CB[6], cucurbit[6]uracil; CS, chondroitin sulfate; ECM, extracellular matrix; RGD, arginine-glycine-aspartic acid; CB[7], cucurbit[7]uril; PCL, poly(caprolactone); PEBA, poly(ether-*b*-amide); UPy, 2-ureido-4[1H]-pyrimidinone; ABS, acrylonitrile-butadiene-styrene; HPMC, hydroxypropyl methylcellulose; DNA, deoxyribonucleic acid; IBMX, 3-isobutyl-1-methylxanthine; NIPAAm, *N*-isopropylacrylamide; NPMAm, *N*-(2-hydroxyproply)methacrylamide; ATMP, amino trimethylene phosphoric acid

REFERENCES

(1) Aida, T.; Meijer, E. W.; Stupp, S. I. Functional Supramolecular Polymers. *Science* **2012**, *335* (6070), 813−817.

(2) Brunsveld, L.; Folmer, B.; Meijer, E.; Sijbesma, R. Supramolecular polymers. *Chem. Rev.* **2001**, *101* (12), 4071−4098.

(3) Li, S.-L.; Xiao, T.; Lin, C.; Wang, L. Advanced supramolecular polymers constructed by orthogonal self-assembly. *Chem. Soc. Rev.* **2012**, *41* (18), 5950−5968.

(4) Faul, C. F.; Antonietti, M. Ionic self-assembly: Facile synthesis of supramolecular materials. *Adv. Mater.* **2003**, *15* (9), 673−683.

(5) Johnson, E. R.; Keinan, S.; Mori-Sanchez, P.; Contreras-Garcia, J.; Cohen, A. J.; Yang, W. Revealing noncovalent interactions. *J. Am. Chem. Soc.* **2010**, *132* (18), 6498−6506.

(6) Odian, G. *Principles of Polymerization*, 4th ed.; Wiley-Interscience: 2004.

(7) Pekkanen, A. M.; Zawaski, C.; Stevenson, A. T., Jr.; Dickerman, R.; Whittington, A. R.; Williams, C. B.; Long, T. E. Poly(ether ester) Ionomers as Water-Soluble Polymers for Material Extrusion Additive Manufacturing Processes. *ACS Appl. Mater. Interfaces* **2017**, *9* (14), 12324−12331.

(8) Schultz, A. R.; Lambert, P. M.; Chartrain, N. A.; Ruohoniemi, D. M.; Zhang, Z.; Jangu, C.; Zhang, M.; Williams, C. B.; Long, T. E. 3D Printing Phosphonium Ionic Liquid Networks with Mask Projection Microstereolithography. *ACS Macro Lett.* **2014**, *3* (11), 1205−1209.

(9) Guvendiren, M.; Molde, J.; Soares, R. M. D.; Kohn, J. Designing biomaterials for 3D printing. *ACS Biomater. Sci. Eng.* **2016**, *2* (10), 1679−1693.

(10) Studart, A. R. Additive manufacturing of biologically-inspired materials. *Chem. Soc. Rev.* **2016**, *45* (2), 359−376.

(11) Stansbury, J. W.; Idacavage, M. J. 3D printing with polymers: Challenges among expanding options and opportunities. *Dent. Mater.* **2016**, *32* (1), 54−64.

(12) Zhang, Z. Z.; Jiang, D.; Ding, J. X.; Wang, S. J.; Zhang, L.; Zhang, J. Y.; Qi, Y. S.; Chen, X. S.; Yu, J. K. Role of scaffold mean pore size in meniscus regeneration. *Acta Biomater.* **2016**, *43*, 314−326.

(13) Murphy, S. V.; Atala, A. 3D bioprinting of tissues and organs. *Nat. Biotechnol.* **2014**, *32* (8), 773−785.

(14) Khademhosseini, A.; Langer, R. Microengineered hydrogels for tissue engineering. *Biomaterials* **2007**, *28* (34), 5087−5092.

(15) Lutolf, M. P.; Hubbell, J. A. Synthetic biomaterials as instructive extracellular microenvironments for morphogenesis in tissue engineering. *Nat. Biotechnol.* **2005**, *23* (1), 47−55.

(16) Kaur, S.; Sandhu, S.; Dhillon, S. K.; Makhni, S. K. Tissue engineering and its future perspective in therapeutic medicine - A brief review. *Journal of Advanced Medical and Dental Sciences Research* **2016**, *4* (4), 159.

(17) Yang, S.; Leong, K.-F.; Du, Z.; Chua, C.-K. The design of scaffolds for use in tissue engineering. Part II. Rapid prototyping techniques. *Tissue Eng.* **2002**, *8* (1), 1−11.

(18) Sears, N.; Dhavalikar, P.; Seshadri, D.; Cosgriff-Hernandez, E. A Review of 3D Printing of Tissue Engineering Constructs. *Tissue Eng., Part B* **2016**, *22* (4), 298−310.

(19) Guven, S.; Chen, P.; Inci, F.; Tasoglu, S.; Erkmen, B.; Demirci, U. Multiscale assembly for tissue engineering and regenerative medicine. *Trends Biotechnol.* **2015**, *33* (5), 269−279.

(20) Lengalova, A.; Vesel, A.; Feng, Y.; Sencadas, V. Biodegradable Polymers for Medical Applications. *Int. J. Polym. Sci.* **2016**, *2016*, 110.1155/2016/6047284

(21) Hubbell, J. A. Biomaterials in tissue engineering. *Nat. Biotechnol.* **1995**, *13* (6), 565−576.

(22) Gunatillake, P. A.; Adhikari, R. Biodegradable synthetic polymers for tissue engineering. *Eur. Cell. Mater.* **2003**, *5* (1), 1−16.

(23) Hutmacher, D. W. Scaffolds in tissue engineering bone and cartilage. *Biomaterials* **2000**, *21* (24), 2529−2543.

(24) Makris, E. A.; Gomoll, A. H.; Malizos, K. N.; Hu, J. C.; Athanasiou, K. A. Repair and tissue engineering techniques for articular cartilage. *Nat. Rev. Rheumatol.* **2015**, *11* (1), 21−34.

(25) Liu, X.; Ma, P. X. Polymeric Scaffolds for Bone Tissue Engineering. *Ann. Biomed. Eng.* **2004**, *32* (3), 477−486.

(26) Yin, X.; Mead, B. E.; Safaee, H.; Langer, R.; Karp, J. M.; Levy, O. Engineering Stem Cell Organoids. *Cell Stem Cell* **2016**, *18* (1), 25−38.

(27) Vogel, V.; Sheetz, M. Local force and geometry sensing regulate cell functions. *Nat. Rev. Mol. Cell Biol.* **2006**, *7* (4), 265−275.

(28) Van Vlierberghe, S.; Dubruel, P.; Schacht, E. Biopolymer-based hydrogels as scaffolds for tissue engineering applications: a review. *Biomacromolecules* **2011**, *12* (5), 1387−1408.

(29) Lewis, P. L.; Shah, R. N. 3D Printing for Liver Tissue Engineering: Current Approaches and Future Challenges. *Current Transplantation Reports* **2016**, *3* (1), 100−108.

(30) Gilmour, A.; Woolley, A.; Poole-Warren, L.; Thomson, C.; Green, R. A critical review of cell culture strategies for modelling intracortical brain implant material reactions. *Biomaterials* **2016**, *91*, 23−43.

(31) Rouwkema, J.; Khademhosseini, A. Vascularization and angiogenesis in tissue engineering: beyond creating static networks. *Trends Biotechnol.* **2016**, *34* (9), 733−745.

(32) Ogle, B. M.; Bursac, N.; Domian, I.; Huang, N. F.; Menasché, P.; Murry, C. E.; Pruitt, B.; Radisic, M.; Wu, J. C.; Wu, S. M. Distilling complexity to advance cardiac tissue engineering. *Sci. Transl. Med.* **2016**, *8* (342), 342ps13−342ps13.

(33) Griffith, L. G.; Naughton, G. Tissue engineering–current challenges and expanding opportunities. *Science* **2002**, *295* (5557), 1009−1014.

(34) Wobma, H.; Vunjak-Novakovic, G. Tissue engineering and regenerative medicine 2015: a year in review. *Tissue Eng., Part B* **2016**, *22* (2), 101−113.

(35) Lim, J. Y.; Donahue, H. J. Cell sensing and response to micro- and nanostructured surfaces produced by chemical and topographic patterning. *Tissue Eng.* **2007**, *13* (8), 1879−1891.

(36) Do, A. V.; Khorsand, B.; Geary, S. M.; Salem, A. K. 3D printing of scaffolds for tissue regeneration applications. *Adv. Healthcare Mater.* **2015**, *4* (12), 1742−1762.

(37) Peterson, G. I.; Schwartz, J. J.; Zhang, D.; Weiss, B.; Ganter, M. A.; Storti, D. W.; Boydston, A. J. Production of Materials with

DOI: 10.1021/acs.biomac.7b00671
Biomacromolecules 2017, 18, 2669−2687

Spatially-Controlled Crosslink Density via Vat Photopolymerization. *ACS Appl. Mater. Interfaces* **2016**, *8* (42), 29037−29043.
(38) Migler, K. *Polymer Additive Manufacturing and Rheology*; NIST: https://www.nist.gov/programs-projects/polymer-additive-manufacturing-and-rheology, 2016.
(39) Jose, R. R.; Rodriguez, M. J.; Dixon, T. A.; Omenetto, F.; Kaplan, D. L. Evolution of Bioinks and Additive Manufacturing Technologies for 3D Bioprinting. *ACS Biomater. Sci. Eng.* **2016**, *2* (10), 1662−1678.
(40) Tang, D.; Tare, R. S.; Yang, L.-Y.; Williams, D. F.; Ou, K.-L.; Oreffo, R. O. C. Biofabrication of bone tissue: approaches, challenges and translation for bone regeneration. *Biomaterials* **2016**, *83*, 363−382.
(41) Carrow, J. K.; Gaharwar, A. K. Bioinspired Polymeric Nanocomposites for Regenerative Medicine. *Macromol. Chem. Phys.* **2015**, *216* (3), 248−264.
(42) Kumar, A.; Mandal, S.; Barui, S.; Vasireddi, R.; Gbureck, U.; Gelinsky, M.; Basu, B. Low temperature additive manufacturing of three dimensional scaffolds for bone-tissue engineering applications: Processing related challenges and property assessment. *Mater. Sci. Eng., R* **2016**, *103*, 1−39.
(43) Sprangers, R.; Velyvis, A.; Kay, L. E. Solution NMR of supramolecular complexes: providing new insights into function. *Nat. Methods* **2007**, *4* (9), 697−703.
(44) *NMR in Supramolecular Chemistry*; Springer Science & Business Media: 2012.
(45) Merino, D. H.; Slark, A. T.; Colquhoun, H. M.; Hayes, W.; Hamley, I. W. Thermo-responsive microphase separated supramolecular polyurethanes. *Polym. Chem.* **2010**, *1* (8), 1263−1271.
(46) Zhang, K.; Chen, M. T.; Drummey, K. J.; Talley, S. J.; Anderson, L. J.; Moore, R. B.; Long, T. E. Ureido cytosine and cytosine-containing acrylic copolymers. *Polym. Chem.* **2016**, *7* (43), 6671−6681.
(47) Burattini, S.; Greenland, B. W.; Hayes, W.; Mackay, M. E.; Rowan, S. J.; Colquhoun, H. M. A Supramolecular Polymer Based on Tweezer-Type pi-pi Stacking Interactions: Molecular Design for Healability and Enhanced Toughness. *Chem. Mater.* **2011**, *23* (1), 6−8.
(48) Yamauchi, K.; Kanomata, A.; Inoue, T.; Long, T. E. Thermoreversible polyesters consisting of multiple hydrogen bonding (MHB). *Macromolecules* **2004**, *37* (10), 3519−3522.
(49) Houston, K. R.; Jackson, A. M. S.; Yost, R. W.; Carman, H. S.; Ashby, V. S. Supramolecular engineering polyesters: endgroup functionalization of glycol modified PET with ureidopyrimidinone. *Polym. Chem.* **2016**, *7* (44), 6744−6751.
(50) Dou, S. C.; Zhang, S. H.; Klein, R. J.; Runt, J.; Colby, R. H. Synthesis and characterization of poly(ethylene glycol)-based single-ion conductors. *Chem. Mater.* **2006**, *18* (18), 4288−4295.
(51) Chen, Q.; Masser, H.; Shiau, H. S.; Liang, S. W.; Runt, J.; Painter, P. C.; Colby, R. H. Linear Viscoelasticity and Fourier Transform Infrared Spectroscopy of Polyether-Ester-Sulfonate Copolymer Ionomers. *Macromolecules* **2014**, *47* (11), 3635−3644.
(52) Webber, M. J.; Appel, E. A.; Meijer, E.; Langer, R. Supramolecular biomaterials. *Nat. Mater.* **2016**, *15* (1), 13−26.
(53) Radhakrishnan, J.; Subramanian, A.; Krishnan, U. M.; Sethuraman, S. Injectable and 3D Bioprinted Polysaccharide Hydrogels: From Cartilage to Osteochondral Tissue Engineering. *Biomacromolecules* **2017**, *18* (1), 1−26.
(54) Necas, J.; Bartosikova, L.; Brauner, P.; Kolar, J. Hyaluronic acid (hyaluronan): a review. *Vet. Med.* **2008**, *53* (8), 397−411.
(55) Collins, M. N.; Birkinshaw, C. Hyaluronic acid based scaffolds for tissue engineering—A review. *Carbohydr. Polym.* **2013**, *92* (2), 1262−1279.
(56) Smeds, K. A.; Grinstaff, M. W. Photocrosslinkable polysaccharides for in situ hydrogel formation. *J. Biomed. Mater. Res.* **2001**, *54* (1), 115−121.
(57) Ouyang, L.; Highley, C. B.; Rodell, C. B.; Sun, W.; Burdick, J. A. 3D Printing of Shear-Thinning Hyaluronic Acid Hydrogels with Secondary Cross-Linking. *ACS Biomater. Sci. Eng.* **2016**, *2* (10), 1743−1751.
(58) Highley, C. B.; Rodell, C. B.; Burdick, J. A. Direct 3D Printing of Shear-Thinning Hydrogels into Self-Healing Hydrogels. *Adv. Mater.* **2015**, *27* (34), 5075−5079.
(59) Skardal, A.; Zhang, J.; Prestwich, G. D. Bioprinting vessel-like constructs using hyaluronan hydrogels crosslinked with tetrahedral polyethylene glycol tetracrylates. *Biomaterials* **2010**, *31* (24), 6173−6181.
(60) Jung, H.; Park, J. S.; Yeom, J.; Selvapalam, N.; Park, K. M.; Oh, K.; Yang, J.-A.; Park, K. H.; Hahn, S. K.; Kim, K. 3D Tissue Engineered Supramolecular Hydrogels for Controlled Chondrogenesis of Human Mesenchymal Stem Cells. *Biomacromolecules* **2014**, *15* (3), 707−714.
(61) Shim, J.-H.; Jang, K.-M.; Hahn, S. K.; Park, J. Y.; Jung, H.; Oh, K.; Park, K. M.; Yeom, J.; Park, S. H.; Kim, S. W. Three-dimensional bioprinting of multilayered constructs containing human mesenchymal stromal cells for osteochondral tissue regeneration in the rabbit knee joint. *Biofabrication* **2016**, *8* (1), 014102.
(62) Wang, D.-A.; Varghese, S.; Sharma, B.; Strehin, I.; Fermanian, S.; Gorham, J.; Fairbrother, D. H.; Cascio, B.; Elisseeff, J. H. Multifunctional chondroitin sulphate for cartilage tissue−biomaterial integration. *Nat. Mater.* **2007**, *6* (5), 385−392.
(63) Abbadessa, A.; Blokzijl, M.; Mouser, V.; Marica, P.; Malda, J.; Hennink, W.; Vermonden, T. A thermo-responsive and photo-polymerizable chondroitin sulfate-based hydrogel for 3D printing applications. *Carbohydr. Polym.* **2016**, *149*, 163−174.
(64) Costantini, M.; Idaszek, J.; Szöke, K.; Jaroszewicz, J.; Dentini, M.; Barbetta, A.; Brinchmann, J. E. Święszkowski, W. 3D bioprinting of BM-MSCs-loaded ECM biomimetic hydrogels for in vitro neocartilage formation. *Biofabrication* **2016**, *8* (3), 035002.
(65) Sun, G.; Shen, Y.-I.; Ho, C. C.; Kusuma, S.; Gerecht, S. Functional groups affect physical and biological properties of dextran-based hydrogels. *J. Biomed. Mater. Res., Part A* **2010**, *93A* (3), 1080−1090.
(66) Pescosolido, L.; Schuurman, W.; Malda, J.; Matricardi, P.; Alhaique, F.; Coviello, T.; van Weeren, P. R.; Dhert, W. J.; Hennink, W. E.; Vermonden, T. Hyaluronic acid and dextran-based semi-IPN hydrogels as biomaterials for bioprinting. *Biomacromolecules* **2011**, *12* (5), 1831−1838.
(67) Grasdalen, H.; Smidsrød, O. Gelation of gellan gum. *Carbohydr. Polym.* **1987**, *7* (5), 371−393.
(68) Lozano, R.; Stevens, L.; Thompson, B. C.; Gilmore, K. J.; Gorkin, R.; Stewart, E. M.; in het Panhuis, M.; Romero-Ortega, M.; Wallace, G. G. 3D printing of layered brain-like structures using peptide modified gellan gum substrates. *Biomaterials* **2015**, *67*, 264−273.
(69) Morris, V. B.; Nimbalkar, S.; Younesi, M.; McClellan, P.; Akkus, O. Mechanical Properties, Cytocompatibility and Manufacturability of Chitosan:PEGDA Hybrid-Gel Scaffolds by Stereolithography. *Ann. Biomed. Eng.* **2017**, *45*, 286−296.
(70) Ng, W. L.; Yeong, W. Y.; Naing, M. W. Polyelectrolyte gelatin-chitosan hydrogel optimized for 3D bioprinting in skin tissue engineering. *Int. J. Bioprinting* **2016**, *2* (1), 10.18063/IJB.2016.01.009.
(71) Müller, W. E.; Tolba, E.; Schröder, H. C.; Neufurth, M.; Wang, S.; Link, T.; Al-Nawas, B.; Wang, X. A new printable and durable N, O-carboxymethyl chitosan−Ca 2+−polyphosphate complex with morphogenetic activity. *J. Mater. Chem. B* **2015**, *3* (8), 1722−1730.
(72) Kuo, C. K.; Ma, P. X. Ionically crosslinked alginate hydrogels as scaffolds for tissue engineering: Part 1. Structure, gelation rate and mechanical properties. *Biomaterials* **2001**, *22* (6), 511−521.
(73) Lee, H.; Hong, S. H.; Ahn, D. J. Stable patterning of sensory agarose gels using inkjet printing. *Macromol. Res.* **2015**, *23* (1), 124−127.
(74) Antoine, E. E.; Vlachos, P. P.; Rylander, M. N. Tunable collagen I hydrogels for engineered physiological tissue micro-environments. *PLoS One* **2015**, *10* (3), e0122500.
(75) Klotz, B. J.; Gawlitta, D.; Rosenberg, A. J.; Malda, J.; Melchels, F. P. Gelatin-Methacryloyl Hydrogels: Towards Biofabrication-Based Tissue Repair. *Trends Biotechnol.* **2016**, *34* (5), 394−407.
(76) Schuurman, W.; Levett, P. A.; Pot, M. W.; van Weeren, P. R.; Dhert, W. J.; Hutmacher, D. W.; Melchels, F. P.; Klein, T. J.; Malda, J.

DOI: 10.1021/acs.biomac.7b00671
Biomacromolecules 2017, 18, 2669−2687

Gelatin-methacrylamide hydrogels as potential biomaterials for fabrication of tissue-engineered cartilage constructs. *Macromol. Biosci.* **2013**, *13* (5), 551−561.
(77) Rutz, A. L.; Hyland, K. E.; Jakus, A. E.; Burghardt, W. R.; Shah, R. N. A Multimaterial Bioink Method for 3D Printing Tunable, Cell-Compatible Hydrogels. *Adv. Mater.* **2015**, *27* (9), 1607−1614.
(78) Hoch, E.; Hirth, T.; Tovar, G. E.; Borchers, K. Chemical tailoring of gelatin to adjust its chemical and physical properties for functional bioprinting. *J. Mater. Chem. B* **2013**, *1* (41), 5675−5685.
(79) Bai, T.; Sun, F.; Zhang, L.; Sinclair, A.; Liu, S.; Ella-Menye, J.-R.; Zheng, Y.; Jiang, S. Restraint of the Differentiation of Mesenchymal Stem Cells by a Nonfouling Zwitterionic Hydrogel. *Angew. Chem., Int. Ed.* **2014**, *53* (47), 12729−12734.
(80) Wang, B.; Benitez, A. J.; Lossada, F.; Merindol, R.; Walther, A. Bioinspired Mechanical Gradients in Cellulose Nanofibril/Polymer Nanopapers. *Angew. Chem., Int. Ed.* **2016**, *55* (20), 5966−5970.
(81) Chen, H.; Hou, S.; Ma, H.; Li, X.; Tan, Y. Controlled gelation kinetics of cucurbit[7]uril-adamantane cross-linked supramolecular hydrogels with competing guest molecules. *Sci. Rep.* **2016**, *6*, 20722.
(82) Censi, R.; Schuurman, W.; Malda, J.; Di Dato, G.; Burgisser, P. E.; Dhert, W. J.; Van Nostrum, C. F.; Di Martino, P.; Vermonden, T.; Hennink, W. E. A Printable Photopolymerizable Thermosensitive p (HPMAm-lactate)-PEG Hydrogel for Tissue Engineering. *Adv. Funct. Mater.* **2011**, *21* (10), 1833−1842.
(83) Hung, K. C.; Tseng, C. S.; Hsu, S. h. Synthesis and 3D Printing of Biodegradable Polyurethane Elastomer by a Water-Based Process for Cartilage Tissue Engineering Applications. *Adv. Healthcare Mater.* **2014**, *3* (10), 1578−1587.
(84) Hung, K.-C.; Tseng, C.-S.; Dai, L.-G.; Hsu, S.-h. Water-based polyurethane 3D printed scaffolds with controlled release function for customized cartilage tissue engineering. *Biomaterials* **2016**, *83*, 156−168.
(85) Gao, L.; Gao, Y.; Lin, Y.; Ju, Y.; Yang, S.; Hu, J. A Charge-Transfer-Induced Self-Healing Supramolecular Hydrogel. *Chem. - Asian J.* **2016**, *11* (23), 3430−3435.
(86) Wei, Q.; Xu, M.; Liao, C.; Wu, Q.; Liu, M.; Zhang, Y.; Wu, C.; Cheng, L.; Wang, Q. Printable hybrid hydrogel by dual enzymatic polymerization with superactivity. *Chem. Sci.* **2016**, *7* (4), 2748−2752.
(87) Wei, Q.; Xu, W.; Liu, M.; Wu, Q.; Cheng, L.; Wang, Q. Viscosity-controlled printing of supramolecular-polymeric hydrogels via dual-enzyme catalysis. *J. Mater. Chem. B* **2016**, *4*, 6302−6306.
(88) Domingos, M.; Chiellini, F.; Gloria, A.; Ambrosio, L.; Bartolo, P.; Chiellini, E. Effect of process parameters on the morphological and mechanical properties of 3D Bioextruded poly(ε-caprolactone) scaffolds. *Rapid Prototyping Journal* **2012**, *18* (1), 56−67.
(89) Hart, L. R.; Li, S.; Sturgess, C.; Wildman, R.; Jones, J. R.; Hayes, W. 3D Printing of Biocompatible Supramolecular Polymers and their Composites. *ACS Appl. Mater. Interfaces* **2016**, *8* (5), 3115−3122.
(90) Dankers, P. Y.; Harmsen, M. C.; Brouwer, L. A.; Van Luyn, M. J.; Meijer, E. A modular and supramolecular approach to bioactive scaffolds for tissue engineering. *Nat. Mater.* **2005**, *4* (7), 568−574.
(91) Chimene, D.; Lennox, K. K.; Kaunas, R. R.; Gaharwar, A. K. Advanced Bioinks for 3D Printing: A Materials Science Perspective. *Ann. Biomed. Eng.* **2016**, *44* (6), 2090−2102.
(92) Chung, R.-J.; Hsieh, M.-F.; Perng, L.-H.; Cheng, Y.-L.; Hsu, T.-J. Meshed Scaffolds Made of a,a′-bis(2-hydroxyethyl methacrylate) poly(ethylene glycol) through 3D Stereolithography. *Biomed. Eng.* **2013**, *25* (05), 1340002.
(93) Jeong, C. G.; Atala, A., 3D Printing and Biofabrication for Load Bearing Tissue Engineering. In *Engineering Mineralized and Load Bearing Tissues*; Springer: 2015; pp 3−14.
(94) Pedde, R. D.; Mirani, B.; Navaei, A.; Styan, T.; Wong, S.; Mehrali, M.; Thakur, A.; Mohtaram, N. K.; Bayati, A.; Dolatshahi-Pirouz, A.; Nikkhah, M.; Willerth, S. M.; Akbari, M. Emerging Biofabrication Strategies for Engineering Complex Tissue Constructs. *Adv. Mater.* **2017**, *29* (19),160606110.1002/adma.201606061
(95) Sears, N. A.; Seshadri, D. R.; Dhavalikar, P. S.; Cosgriff-Hernandez, E. A Review of Three-Dimensional Printing in Tissue Engineering. *Tissue Eng., Part B* **2016**, *22* (4), 298−310.
(96) Bajaj, P.; Schweller, R. M.; Khademhosseini, A.; West, J. L.; Bashir, R. 3D biofabrication strategies for tissue engineering and regenerative medicine. *Annu. Rev. Biomed. Eng.* **2014**, *16*, 247−76.
(97) Annabi, N.; Nichol, J. W.; Zhong, X.; Ji, C. D.; Koshy, S.; Khademhosseini, A.; Dehghani, F. Controlling the Porosity and Microarchitecture of Hydrogels for Tissue Engineering. *Tissue Eng., Part B* **2010**, *16* (4), 371−383.
(98) Melchels, F. P. W.; Feijen, J.; Grijpma, D. W. A review on stereolithography and its applications in biomedical engineering. *Biomaterials* **2010**, *31* (24), 6121−6130.
(99) Peltola, S. M.; Melchels, F. P. W.; Grijpma, D. W.; Kellomaki, M. A review of rapid prototyping techniques for tissue engineering purposes. *Ann. Med.* **2008**, *40* (4), 268−280.
(100) Mondschein, R. J.; Kanitkar, A.; Williams, C. B.; Verbridge, S. S.; Long, T. E. Polymer structure-property requirements for stereolithographic 3D printing of soft tissue engineering scaffolds. *Biomaterials* **2017**, *140*, 170−188.
(101) Akkineni, A. R.; Ahlfeld, T.; Funk, A.; Waske, A.; Lode, A.; Gelinsky, M. Highly Concentrated Alginate-Gellan Gum Composites for 3D Plotting of Complex Tissue Engineering Scaffolds. *Polymers* **2016**, *8* (5), 170.
(102) Mouser, V. H.; Melchels, F. P.; Visser, J.; Dhert, W. J.; Gawlitta, D.; Malda, J. Yield stress determines bioprintability of hydrogels based on gelatin-methacryloyl and gellan gum for cartilage bioprinting. *Biofabrication* **2016**, *8* (3), 035003.
(103) Keller, A.; Stevens, L.; Wallace, G. G. 3D Printed Edible Hydrogel Electrodes. *MRS Adv.* **2016**, *1* (08), 527−532.
(104) Liu, Y.; Liu, Y.; Hamid, Q.; Hamid, Q.; Snyder, J.; Snyder, J.; Wang, C.; Wang, C.; Sun, W.; Sun, W. Evaluating fabrication feasibility and biomedical application potential of in situ 3D printing technology. *Rapid Prototyping Journal* **2016**, *22* (6), 947−955.
(105) Stein, N.; Saathoff, T.; Antoni, S.-T.; Schlaefer, A. Creating 3D gelatin phantoms for experimental evaluation in biomedicine. *Current Directions in Biomedical Engineering* **2015**, *1* (1), 331−334.
(106) Rodriguez, M. J.; Brown, J.; Giordano, J.; Lin, S. J.; Omenetto, F. G.; Kaplan, D. L. Silk based bioinks for soft tissue reconstruction using 3-dimensional (3D) printing with in vitro and in vivo assessments. *Biomaterials* **2016**, *117*, 105−115.
(107) Ahlfeld, T.; Akkineni, A. R.; Förster, Y.; Köhler, T.; Knaack, S.; Gelinsky, M.; Lode, A. Design and fabrication of complex scaffolds for bone defect healing: combined 3D plotting of a calcium phosphate cement and a growth factor-loaded hydrogel. *Ann. Biomed. Eng.* **2017**, *45*, 1−13.
(108) Lin, K.-F.; He, S.; Song, Y.; Wang, C.-M.; Gao, Y.; Li, J.-Q.; Tang, P.; Wang, Z.; Bi, L.; Pei, G.-X. Low-Temperature Additive Manufacturing of Biomimic Three-Dimensional Hydroxyapatite/Collagen Scaffolds for Bone Regeneration. *ACS Appl. Mater. Interfaces* **2016**, *8* (11), 6905−6916.
(109) Lode, A.; Meyer, M.; Brüggemeier, S.; Paul, B.; Baltzer, H.; Schröpfer, M.; Winkelmann, C.; Sonntag, F.; Gelinsky, M. Additive manufacturing of collagen scaffolds by three-dimensional plotting of highly viscous dispersions. *Biofabrication* **2016**, *8* (1), 015015.
(110) Akkineni, A. R.; Ahlfeld, T.; Lode, A.; Gelinsky, M. A versatile method for combining different biopolymers in a core/shell fashion by 3D plotting to achieve mechanically robust constructs. *Biofabrication* **2016**, *8* (4), 045001.
(111) Khaled, S. A.; Burley, J. C.; Alexander, M. R.; Roberts, C. J. Desktop 3D printing of controlled release pharmaceutical bilayer tablets. *Int. J. Pharm.* **2014**, *461* (1−2), 105−111.
(112) Pietrzak, K.; Isreb, A.; Alhnan, M. A. A flexible-dose dispenser for immediate and extended release 3D printed tablets. *Eur. J. Pharm. Biopharm.* **2015**, *96*, 380−387.
(113) Albarahmieh, E.; Qia, S.; Craig, D. Hot Melt Extruded Transdermal Films based on Amorphous Solid Dispersions in Eudragit RS PO: The Inclusion of Hydrophilic Additives to Develop Moisture-Activated Release Systems. *Int. J. Pharm.* **2016**, *514* (1), 270−281.
(114) Zhang, F. Melt-Extruded Eudragit® FS-Based Granules for Colonic Drug Delivery. *AAPS PharmSciTech* **2016**, *17* (1), 56−67.

DOI: 10.1021/acs.biomac.7b00671
Biomacromolecules 2017, 18, 2669−2687

(115) Nernplod, T.; Akkaramongkolporn, P.; Sriamornsak, P. In Preparation of Eudragit® L Beads for Intragastric Floating Drug Delivery. *Adv. Mater. Res.*; Trans Tech Publ: 2015; pp 79−82.
(116) Vo, A. Q.; Feng, X.; Morott, J. T.; Pimparade, M. B.; Tiwari, R. V.; Zhang, F.; Repka, M. A. A novel floating controlled release drug delivery system prepared by hot-melt extrusion. *Eur. J. Pharm. Biopharm.* **2016**, *98*, 108−121.
(117) Vogler, E. A. Protein adsorption in three dimensions. *Biomaterials* **2012**, *33* (5), 1201−1237.
(118) Nesti, L. J.; Li, W.-J.; Shanti, R. M.; Jiang, Y. J.; Jackson, W.; Freedman, B. A.; Kuklo, T. R.; Giuliani, J. R.; Tuan, R. S. Intervertebral disc tissue engineering using a novel hyaluronic acid−nanofibrous scaffold (HANFS) amalgam. *Tissue Eng., Part A* **2008**, *14* (9), 1527−1537.
(119) Yang, Y.; Chen, Y.; Wei, Y.; Li, Y. 3D printing of shape memory polymer for functional part fabrication. *Int. J. Adv. Manuf. Technol.* **2016**, *84*, 2079−2095.
(120) Zhu, F.; Cheng, L.; Yin, J.; Wu, Z.; Qian, J.; Fu, J.; Zheng, Q. 3D printing of ultra-tough polyion complex hydrogels. *ACS Appl. Mater. Interfaces* **2016**, *8* (45), 31304−31310.
(121) Maher, P.; Keatch, R.; Donnelly, K.; Mackay, R.; Paxton, J. Construction of 3D biological matrices using rapid prototyping technology. *Rapid Prototyping Journal* **2009**, *15* (3), 204−210.
(122) Boere, K. W. M.; Visser, J.; Seyednejad, H.; Rahimian, S.; Gawlitta, D.; van Steenbergen, M. J.; Dhert, W. J. A.; Hennink, W. E.; Vermonden, T.; Malda, J. Covalent attachment of a three-dimensionally printed Thermoplast to a gelatin hydrogel for mechanically enhanced cartilage constructs. *Acta Biomater.* **2014**, *10* (6), 2602−2611.
(123) Hong, S.; Sycks, D.; Chan, H. F.; Lin, S.; Lopez, G. P.; Guilak, F.; Leong, K. W.; Zhao, X. 3D printing of highly stretchable and tough hydrogels into complex, cellularized structures. *Adv. Mater.* **2015**, *27* (27), 4035−4040.
(124) Bakarich, S. E.; Beirne, S.; Wallace, G. G.; Spinks, G. M. Extrusion printing of ionic−covalent entanglement hydrogels with high toughness. *J. Mater. Chem. B* **2013**, *1* (38), 4939−4946.
(125) Allen, P. B.; Khaing, Z.; Schmidt, C. E.; Ellington, A. D. 3D Printing with Nucleic Acid Adhesives. *ACS Biomater. Sci. Eng.* **2015**, *1* (1), 19−26.
(126) Skoog, S. A.; Goering, P. L.; Narayan, R. J. Stereolithography in tissue engineering. *J. Mater. Sci.: Mater. Med.* **2014**, *25* (3), 845−856.
(127) Pal, K.; Sagiri, S. S.; Singh, V. K.; Behera, B.; Banerjee, I.; Pramanik, K. Natural Polymers: Tissue Engineering. *Drug delivery* **2015**, *39*, 40.
(128) Elomaa, L.; Pan, C.-C.; Shanjani, Y.; Malkovskiy, A.; Seppala, J. V.; Yang, Y. Three-dimensional fabrication of cell-laden biodegradable poly(ethylene glycol-co-depsipeptide) hydrogels by visible light stereolithography. *J. Mater. Chem. B* **2015**, *3* (42), 8348−8358.
(129) Fedorovich, N. E.; Swennen, I.; Girones, J.; Moroni, L.; Van Blitterswijk, C. A.; Schacht, E.; Alblas, J.; Dhert, W. J. Evaluation of photocrosslinked lutrol hydrogel for tissue printing applications. *Biomacromolecules* **2009**, *10* (7), 1689−1696.
(130) Pyo, S.-H.; Wang, P.; Zhu, W.; Hwang, H.; Warner, J. J.; Chen, S. Continuous Optical 3D Printing of Green Aliphatic Polyurethanes. *ACS Appl. Mater. Interfaces* **2017**, *9* (1), 836−844.
(131) Petrochenko, P. E.; Torgersen, J.; Gruber, P.; Hicks, L. A.; Zheng, J.; Kumar, G.; Narayan, R. J.; Goering, P. L.; Liska, R.; Stampfl, J. Laser 3D printing with sub-microscale resolution of porous elastomeric scaffolds for supporting human bone stem cells. *Adv. Healthcare Mater.* **2015**, *4* (5), 739−747.
(132) Sirrine, J. M.; Pekkanen, A. M.; Nelson, A. M.; Chartrain, N. A.; Williams, C. B.; Long, T. E. 3D-printable biodegradable polyester tissue scaffolds for cell adhesion. *Aust. J. Chem.* **2015**, *68* (9), 1409−1414.
(133) Yue, J.; Zhao, P.; Gerasimov, J. Y.; van de Lagemaat, M.; Grotenhuis, A.; Rustema-Abbing, M.; van der Mei, H. C.; Busscher, H. J.; Herrmann, A.; Ren, Y. 3D-Printable Antimicrobial Composite Resins. *Adv. Funct. Mater.* **2015**, *25* (43), 6756−6767.
(134) Zawko, S. A.; Suri, S.; Truong, Q.; Schmidt, C. E. Photopatterned anisotropic swelling of dual-crosslinked hyaluronic acid hydrogels. *Acta Biomater.* **2009**, *5* (1), 14−22.
(135) Suri, S.; Schmidt, C. E. Photopatterned collagen−hyaluronic acid interpenetrating polymer network hydrogels. *Acta Biomater.* **2009**, *5* (7), 2385−2397.
(136) Gonçalves, J. L. D. S.; Valandro, S. R.; Wu, H.-F.; Lee, Y.-H.; Mettra, B.; Monnereau, C.; Cavalheiro, C. C. S.; Pawlicka, A.; Focsan, M.; Lin, C.-L. In *3D printing of natural organic materials by photochemistry*; SPIE OPTO, International Society for Optics and Photonics: 2016; pp 97450E−97450E-7.
(137) Placone, J. K.; Navarro, J.; Laslo, G. W.; Lerman, M. J.; Gabard, A. R.; Herendeen, G. J.; Falco, E. E.; Tomblyn, S.; Burnett, L.; Fisher, J. P. Development and Characterization of a 3D Printed, Keratin-Based Hydrogel. *Ann. Biomed. Eng.* **2017**, *45*, 237−248.
(138) Pawar, A. A.; Saada, G.; Cooperstein, I.; Larush, L.; Jackman, J. A.; Tabaei, S. R.; Cho, N.-J.; Magdassi, S. High-performance 3D printing of hydrogels by water-dispersible photoinitiator nanoparticles. *Sci. Adv.* **2016**, *2* (4), e1501381.
(139) Lee, J. M.; Yeong, W. Y. Design and Printing Strategies in 3D Bioprinting of Cell-Hydrogels: A Review. *Adv. Healthcare Mater.* **2016**, *5* (22), 2856−2865.
(140) Yeo, M.; Ha, J.; Lee, H.; Kim, G. Fabrication of hASCs-laden structures using extrusion-based cell printing supplemented with an electric field. *Acta Biomater.* **2016**, *38*, 33−43.
(141) Kani, M. H.; Chan, E.-C.; Young, R. C.; Butler, T.; Smith, R.; Paul, J. W. 3D Cell Culturing and Possibilities for Myometrial Tissue Engineering. *Ann. Biomed. Eng.* **2017**, *45*, 1746−1757.
(142) Vanderburgh, J.; Sterling, J. A.; Guelcher, S. A. 3D Printing of Tissue Engineered Constructs for In Vitro Modeling of Disease Progression and Drug Screening. *Ann. Biomed. Eng.* **2017**, *45*, 164−179.
(143) Markstedt, K.; Mantas, A.; Tournier, I.; Martínez Ávila, H. c.; Hägg, D.; Gatenholm, P. 3D bioprinting human chondrocytes with nanocellulose−alginate bioink for cartilage tissue engineering applications. *Biomacromolecules* **2015**, *16* (5), 1489−1496.
(144) Das, S.; Pati, F.; Chameettachal, S.; Pahwa, S.; Ray, A. R.; Dhara, S.; Ghosh, S. Enhanced redifferentiation of chondrocytes on microperiodic silk/gelatin scaffolds: toward tailor-made tissue engineering. *Biomacromolecules* **2013**, *14* (2), 311−321.
(145) Yeo, M.; Lee, J.-S.; Chun, W.; Kim, G. H. An Innovative Collagen-Based Cell-Printing Method for Obtaining Human Adipose Stem Cell-Laden Structures Consisting of Core−Sheath Structures for Tissue Engineering. *Biomacromolecules* **2016**, *17* (4), 1365−1375.
(146) Gurkan, U. A.; El Assal, R.; Yildiz, S. E.; Sung, Y.; Trachtenberg, A. J.; Kuo, W. P.; Demirci, U. Engineering Anisotropic Biomimetic Fibrocartilage Microenvironment by Bioprinting Mesenchymal Stem Cells in Nanoliter Gel Droplets. *Mol. Pharmaceutics* **2014**, *11* (7), 2151−2159.
(147) Gao, G.; Yonezawa, T.; Hubbell, K.; Dai, G.; Cui, X. Inkjet-bioprinted acrylated peptides and PEG hydrogel with human mesenchymal stem cells promote robust bone and cartilage formation with minimal printhead clogging. *Biotechnol. J.* **2015**, *10* (10), 1568−1577.
(148) Koch, L.; Deiwick, A.; Schlie, S.; Michael, S.; Gruene, M.; Coger, V.; Zychlinski, D.; Schambach, A.; Reimers, K.; Vogt, P. M. Skin tissue generation by laser cell printing. *Biotechnol. Bioeng.* **2012**, *109* (7), 1855−1863.
(149) Pourchet, L. J.; Thepot, A.; Albouy, M.; Courtial, E. J.; Boher, A.; Blum, L. J.; Marquette, C. A. Human Skin 3D Bioprinting Using Scaffold-Free Approach. *Adv. Healthcare Mater.* **2017**, *6* (4), 1601101.
(150) Lee, H.; Han, W.; Kim, H.; Ha, D.-H.; Jang, J.; Kim, B. S.; Cho, D.-W. Development of Liver Decellularized Extracellular Matrix Bioink for Three-Dimensional Cell Printing-Based Liver Tissue Engineering. *Biomacromolecules* **2017**, *18* (4), 1229−1237.
(151) Xu, M.; Wang, X.; Yan, Y.; Yao, R.; Ge, Y. An cell-assembly derived physiological 3D model of the metabolic syndrome, based on adipose-derived stromal cells and a gelatin/alginate/fibrinogen matrix. *Biomaterials* **2010**, *31* (14), 3868−3877.

DOI: 10.1021/acs.biomac.7b00671
Biomacromolecules 2017, 18, 2669−2687

(152) Billiet, T.; Gevaert, E.; De Schryver, T.; Cornelissen, M.; Dubruel, P. The 3D printing of gelatin methacrylamide cell-laden tissue-engineered constructs with high cell viability. *Biomaterials* **2014**, *35* (1), 49−62.
(153) Homan, K. A.; Kolesky, D. B.; Skylar-Scott, M. A.; Herrmann, J.; Obuobi, H.; Moisan, A.; Lewis, J. A. Bioprinting of 3D Convoluted Renal Proximal Tubules on Perfusable Chips. *Sci. Rep.* **2016**, *6*, 34845.
(154) Kinstlinger, I. S.; Miller, J. S. 3D-printed fluidic networks as vasculature for engineered tissue. *Lab Chip* **2016**, *16* (11), 2025−2043.
(155) Guillotin, B.; Souquet, A.; Catros, S.; Duocastella, M.; Pippenger, B.; Bellance, S.; Bareille, R.; Rémy, M.; Bordenave, L.; Amédée, J. Laser assisted bioprinting of engineered tissue with high cell density and microscale organization. *Biomaterials* **2010**, *31* (28), 7250−7256.
(156) Lee, J. W.; Choi, Y.-J.; Yong, W.-J.; Pati, F.; Shim, J.-H.; Kang, K. S.; Kang, I.-H.; Park, J.; Cho, D.-W. Development of a 3D cell printed construct considering angiogenesis for liver tissue engineering. *Biofabrication* **2016**, *8* (1), 015007.
(157) Duan, B.; Hockaday, L. A.; Kang, K. H.; Butcher, J. T. 3D Bioprinting of heterogeneous aortic valve conduits with alginate/gelatin hydrogels. *J. Biomed. Mater. Res., Part A* **2013**, *101A* (5), 1255−1264.
(158) Hockaday, L.; Kang, K.; Colangelo, N.; Cheung, P.; Duan, B.; Malone, E.; Wu, J.; Girardi, L.; Bonassar, L.; Lipson, H. Rapid 3D printing of anatomically accurate and mechanically heterogeneous aortic valve hydrogel scaffolds. *Biofabrication* **2012**, *4* (3), 035005.
(159) Hölzl, K.; Lin, S.; Tytgat, L.; Van Vlierberghe, S.; Gu, L.; Ovsianikov, A. Bioink properties before, during and after 3D bioprinting. *Biofabrication* **2016**, *8* (3), 032002.
(160) Cubo, N.; Garcia, M.; del Cañizo, J. F.; Velasco, D.; Jorcano, J. L. 3D bioprinting of functional human skin: production and in vivo analysis. *Biofabrication* **2017**, *9* (1), 015006.
(161) Bhuthalingam, R.; Lim, P. Q.; Irvine, S. A.; Agrawal, A.; Mhaisalkar, P. S.; An, J.; Chua, C. K.; Venkatraman, S. A novel 3D printing method for cell alignment and differentiation. *Int. J. Bioprint.* **2015**, *1* (1).10.18063/IJB.2015.01.008
(162) Huang, S.; Yao, B.; Xie, J.; Fu, X. 3D bioprinted extracellular matrix mimics facilitate directed differentiation of epithelial progenitors for sweat gland regeneration. *Acta Biomater.* **2016**, *32*, 170−177.
(163) Arai, K.; Tsukamoto, Y.; Yoshida, H.; Sanae, H.; Mir, T. A.; Sakai, S.; Yoshida, T.; Okabe, M.; Nikaido, T.; Taya, M. The development of cell-adhesive hydrogel for 3D printing. *Int. J. Bioprint.* **2016**, *2* (2), 153−16210.18063/IJB.2016.02.002.
(164) Kesti, M.; Müller, M.; Becher, J.; Schnabelrauch, M.; D'Este, M.; Eglin, D.; Zenobi-Wong, M. A versatile bioink for three-dimensional printing of cellular scaffolds based on thermally and photo-triggered tandem gelation. *Acta Biomater.* **2015**, *11*, 162−172.
(165) You, F.; Wu, X.; Zhu, N.; Lei, M.; Eames, B. F.; Chen, X. 3D Printing of Porous Cell-Laden Hydrogel Constructs for Potential Applications in Cartilage Tissue Engineering. *ACS Biomater. Sci. Eng.* **2016**, *2* (7), 1200−1210.
(166) Kang, H.-W.; Lee, S. J.; Ko, I. K.; Kengla, C.; Yoo, J. J.; Atala, A. A 3D bioprinting system to produce human-scale tissue constructs with structural integrity. *Nat. Biotechnol.* **2016**, *34* (3), 312−319.
(167) Kundu, J.; Shim, J. H.; Jang, J.; Kim, S. W.; Cho, D. W. An additive manufacturing-based PCL−alginate−chondrocyte bioprinted scaffold for cartilage tissue engineering. *J. Tissue Eng. Regener. Med.* **2015**, *9* (11), 1286−1297.
(168) Abbadessa, A.; Mouser, V. H.; Blokzijl, M. M.; Gawlitta, D.; Dhert, W. J.; Hennink, W. E.; Malda, J.; Vermonden, T. A synthetic thermo-sensitive hydrogel for cartilage bioprinting and its biofunctionalization with polysaccharides. *Biomacromolecules* **2016**, *17* (6), 2137−2147.
(169) Yang, L.; Shridhar, S. V.; Gerwitz, M.; Soman, P. An in vitro vascular chip using 3D printing-enabled hydrogel casting. *Biofabrication* **2016**, *8* (3), 035015.
(170) Du, M.; Chen, B.; Meng, Q.; Liu, S.; Zheng, X.; Zhang, C.; Wang, H.; Li, H.; Wang, N.; Dai, J. 3D bioprinting of BMSC-laden methacrylamide gelatin scaffolds with CBD-BMP2-collagen microfibers. *Biofabrication* **2015**, *7* (4), 044104.
(171) Kolesky, D. B.; Homan, K. A.; Skylar-Scott, M. A.; Lewis, J. A. Three-dimensional bioprinting of thick vascularized tissues. *Proc. Natl. Acad. Sci. U. S. A.* **2016**, *113* (12), 3179−3184.
(172) Park, J. Y.; Shim, J.-H.; Choi, S.-A.; Jang, J.; Kim, M.; Lee, S. H.; Cho, D.-W. 3D printing technology to control BMP-2 and VEGF delivery spatially and temporally to promote large-volume bone regeneration. *J. Mater. Chem. B* **2015**, *3* (27), 5415−5425.
(173) Huang, J.; Fu, H.; Wang, Z.; Meng, Q.; Liu, S.; Wang, H.; Zheng, X.; Dai, J.; Zhang, Z. BMSCs-laden gelatin/sodium alginate/carboxymethyl chitosan hydrogel for 3D bioprinting. *RSC Adv.* **2016**, *6* (110), 108423−108430.
(174) Das, S.; Pati, F.; Choi, Y.-J.; Rijal, G.; Shim, J.-H.; Kim, S. W.; Ray, A. R.; Cho, D.-W.; Ghosh, S. Bioprintable, cell-laden silk fibroin−gelatin hydrogel supporting multilineage differentiation of stem cells for fabrication of three-dimensional tissue constructs. *Acta Biomater.* **2015**, *11*, 233−246.
(175) Liu, J.; Hwang, H. H.; Wang, P.; Whang, G.; Chen, S. Direct 3D-printing of cell-laden constructs in microfluidic architectures. *Lab Chip* **2016**, *16* (8), 1430−1438.
(176) Ouyang, L.; Yao, R.; Zhao, Y.; Sun, W. Effect of bioink properties on printability and cell viability for 3D bioplotting of embryonic stem cells. *Biofabrication* **2016**, *8* (3), 035020.
(177) Zhao, X.; Du, S.; Chai, L.; Xu, Y.; Liu, L.; Zhou, X.; Wang, J.; Zhang, W.; Liu, C.-H.; Wang, X. Anti-cancer drug screening based on a adipose-derived stem cell/hepatocyte 3D printing technique. *J. Stem Cell Res. Ther.* **2015**, *2015*.
(178) Wang, X.-F.; Lu, P.-J.; Song, Y.; Sun, Y.-C.; Wang, Y.-G.; Wang, Y. Nano hydroxyapatite particles promote osteogenesis in a three-dimensional bio-printing construct consisting of alginate/gelatin/hASCs. *RSC Adv.* **2016**, *6* (8), 6832−6842.
(179) Kim, Y. B.; Lee, H.; Kim, G. H. Strategy to Achieve Highly Porous/Biocompatible Macroscale Cell Blocks, Using a Collagen/Genipin-bioink and an Optimal 3D Printing Process. *ACS Appl. Mater. Interfaces* **2016**, *8* (47), 32230−32240.
(180) Dai, X.; Ma, C.; Lan, Q.; Xu, T. 3D bioprinted glioma stem cells for brain tumor model and applications of drug susceptibility. *Biofabrication* **2016**, *8* (4), 045005.
(181) England, S.; Rajaram, A.; Schreyer, D. J.; Chen, X. Bioprinted fibrin-factor XIII-hyaluronate hydrogel scaffolds with encapsulated Schwann cells and their in vitro characterization for use in nerve regeneration. *Bioprinting* **2017**, *5*, 1−9.
(182) Schirmer, K. S.; Gorkin, R., III; Beirne, S.; Stewart, E.; Thompson, B. C.; Quigley, A. F.; Kapsa, R. M.; Wallace, G. G. Cell compatible encapsulation of filaments into 3D hydrogels. *Biofabrication* **2016**, *8* (2), 025013.
(183) Gu, Q.; Tomaskovic-Crook, E.; Lozano, R.; Chen, Y.; Kapsa, R. M.; Zhou, Q.; Wallace, G. G.; Crook, J. M. Functional 3D Neural Mini-Tissues from Printed Gel-Based Bioink and Human Neural Stem Cells. *Adv. Healthcare Mater.* **2016**, *5* (12), 1429−1438.
(184) Li, C.; Faulkner-Jones, A.; Dun, A. R.; Jin, J.; Chen, P.; Xing, Y.; Yang, Z.; Li, Z.; Shu, W.; Liu, D. Rapid Formation of a Supramolecular Polypeptide−DNA Hydrogel for In Situ Three-Dimensional Multilayer Bioprinting. *Angew. Chem., Int. Ed.* **2015**, *54* (13), 3957−3961.
(185) Irvine, S. A.; Agrawal, A.; Lee, B. H.; Chua, H. Y.; Low, K. Y.; Lau, B. C.; Machluf, M.; Venkatraman, S. Printing cell-laden gelatin constructs by free-form fabrication and enzymatic protein crosslinking. *Biomed. Microdevices* **2015**, *17* (1), 1−8.
(186) Ouyang, L.; Yao, R.; Chen, X.; Na, J.; Sun, W. 3D printing of HEK 293FT cell-laden hydrogel into macroporous constructs with high cell viability and normal biological functions. *Biofabrication* **2015**, *7* (1), 015010.
(187) Zhang, K.; Fu, Q.; Yoo, J.; Chen, X.; Chandra, P.; Mo, X.; Song, L.; Atala, A.; Zhao, W. 3D bioprinting of urethra with PCL/PLCL blend and dual autologous cells in fibrin hydrogel: an in vitro evaluation of biomimetic mechanical property and cell growth environment. *Acta Biomater.* **2017**, *50*, 154−164.

DOI: 10.1021/acs.biomac.7b00671
Biomacromolecules 2017, 18, 2669−2687

(188) Parker, P.; Moya, M.; Wheeler, E. *Development and Optimization of Viable Human Platforms through 3D Printing*; Lawrence Livermore National Laboratory (LLNL): Livermore, CA, https://e-reports-ext.llnl.gov/pdf/799294.pdf, 2015.
(189) Gaetani, R.; Feyen, D. A.; Verhage, V.; Slaats, R.; Messina, E.; Christman, K. L.; Giacomello, A.; Doevendans, P. A.; Sluijter, J. P. Epicardial application of cardiac progenitor cells in a 3D-printed gelatin/hyaluronic acid patch preserves cardiac function after myocardial infarction. *Biomaterials* **2015**, *61*, 339−348.
(190) Wei, J.; Wang, J.; Su, S.; Wang, S.; Qiu, J.; Zhang, Z.; Christopher, G.; Ning, F.; Cong, W. 3D printing of an extremely tough hydrogel. *RSC Adv.* **2015**, *5* (99), 81324−81329.
(191) Egan, P.; Ferguson, S. J.; Shea, K. Design and 3D printing of hierarchical tissue engineering scaffolds based on mechanics and biology perspectives. *Proceedings of the 28th International Conference on Design Theory and Methodology* **2016**, 24.
(192) Dimas, L. S.; Bratzel, G. H.; Eylon, I.; Buehler, M. J. Tough Composites Inspired by Mineralized Natural Materials: Computation, 3D printing, and Testing. *Adv. Funct. Mater.* **2013**, *23* (36), 4629−4638.
(193) Tibbitt, M. W.; Rodell, C. B.; Burdick, J. A.; Anseth, K. S. Progress in material design for biomedical applications. *Proc. Natl. Acad. Sci. U. S. A.* **2015**, *112* (47), 14444−14451.
(194) Zhu, M.; Li, K.; Zhu, Y.; Zhang, J.; Ye, X. 3D-printed hierarchical scaffold for localized isoniazid/rifampin drug delivery and osteoarticular tuberculosis therapy. *Acta Biomater.* **2015**, *16*, 145−155.
(195) Dou, P.; Liu, Z.; Cao, Z.; Zheng, J.; Wang, C.; Xu, X. Rapid synthesis of hierarchical nanostructured Polyaniline hydrogel for high power density energy storage application and three-dimensional multilayers printing. *J. Mater. Sci.* **2016**, *51* (9), 4274−4282.
(196) Loo, Y.; Lakshmanan, A.; Ni, M.; Toh, L. L.; Wang, S.; Hauser, C. A. Peptide bioink: self-assembling nanofibrous scaffolds for three-dimensional organotypic cultures. *Nano Lett.* **2015**, *15* (10), 6919−6925.

DOI: 10.1021/acs.biomac.7b00671
Biomacromolecules 2017, 18, 2669−2687